# Geologic Map of the Woodland Quadrangle, Clark and Cowlitz Counties, Washington

By Russell C. Evarts

Pamphlet to accompany
Scientific Investigations Map 2827

125 years of science for America 1879–2004

2004

U.S. Department of the Interior
U.S. Geological Survey

# INTRODUCTION

## GEOGRAPHIC AND GEOLOGIC SETTING

The Woodland 7.5' quadrangle is situated in the Puget-Willamette Lowland approximately 50 km north of Portland, Oregon (fig. 1). The lowland, which extends from Puget Sound into west-central Oregon, is a complex structural and topographic trough that lies between the Coast Range and the Cascade Range. Since late Eocene time, the Cascade Range has been the locus of an active volcanic arc associated with underthrusting of oceanic lithosphere beneath the North American continent along the Cascadia Subduction Zone. The Coast Range occupies the forearc position within the Cascadia arc-trench system and consists of a complex assemblage of Eocene to Miocene volcanic and marine sedimentary rocks.

The Woodland quadrangle lies at the northern edge of the Portland Basin, a roughly 2000-km$^2$ topographic and structural depression that is the northernmost of several sediment-filled structural basins, which collectively constitute the Willamette Valley segment of the Puget-Willamette Lowland (Beeson and others, 1989; Swanson and others, 1993; Yeats and others, 1996). The Portland Basin is approximately 70 km long and 30 km wide; its long dimension is oriented northwest. Its northern boundary coincides, in part, with the lower Lewis River, which flows westward through the center of the quadrangle. The Lewis drains a large area in the southern Washington Cascade Range, including the southern flank of Mount St. Helens approximately 25 km upstream from the quadrangle, and joins the Columbia River about 6 km south of Woodland (fig. 1). Northwest of Woodland, the Columbia River exits the broad floodplain of the Portland Basin and flows northward through a relatively narrow bedrock valley at an elevation near sea level. The flanks of the Portland Basin consist of Eocene through Miocene volcanic and sedimentary rocks that rise to elevations exceeding 2000 ft (610 m). Seismic-reflection profiles (L.M. Liberty, written commun., 2003) and lithologic logs of water wells (Swanson and others, 1993; Mabey and Madin, 1995) indicate that as much as 550 m of late Miocene and younger sediments have accumulated in the deepest part of the basin near Vancouver. Most of this basin-fill material was carried in from the east by the Columbia River but sediment deposited by streams draining the adjacent highlands are locally important.

The Portland Basin has been interpreted as a pull-apart basin located in the releasing stepover between two en echelon, northwest-striking, right-lateral fault zones (Beeson and others, 1985, 1989; Beeson and Tolan, 1990; Yelin and Patton, 1991; Blakely and others, 1995). These fault zones are thought to reflect regional transpression and dextral shear within the forearc in response to oblique subduction of the Pacific Plate along the Cascadia Subduction Zone (Pezzopane and Weldon, 1993; Wells and others, 1998). The southwestern margin of the Portland Basin is a well-defined topographic break along the base of the Tualatin Mountains, an asymmetric anticlinal ridge that is bounded on its northeast flank by the Portland Hills Fault Zone (Balsillie and Benson, 1971; Beeson and others, 1989; Blakely and others, 1995), which is probably an active structure (Wong and others, 2001; Liberty and others, 2003). The nature of the corresponding northeastern margin of the basin is less clear, but a poorly defined and partially buried dextral extensional fault zone has been hypothesized from topography, microseismicity, potential field-anomalies, and reconnaissance geologic mapping (Beeson and others, 1989; Beeson and Tolan, 1990; Yelin and Patton, 1991; Blakely and others, 1995). Another dextral structure may control the north-northwest-trending reach of the Columbia River between Portland and Longview (Blakely and others, 1995; Evarts, 2002; Evarts and others, 2002).

This map is a contribution to a U.S. Geological Survey program designed to improve the geologic database for the Portland Basin part of the Pacific Northwest urban corridor, the densely populated Cascadia forearc region of western Washington and Oregon. Better and more detailed information on the bedrock and surficial geology of the basin and its surrounding area is needed to refine assessments of seismic risk (Yelin and Patton, 1991; Bott and Wong, 1993), ground-failure hazards (Madin and Wang, 1999; Wegmann and Walsh, 2001) and resource availability in this rapidly growing region. The digital database for this publication is available on the World Wide Web at http://pubs.usgs.gov/sim/2004/2827.

## PREVIOUS GEOLOGIC INVESTIGATIONS

Previous geologic mapping in the Woodland area, generally carried out as part of broad regional reconnaissance investigations, established the basic stratigraphic framework and distribution of geologic units in the quadrangle. The area directly west of the Woodland quadrangle was mapped at a scale of 1:62,500 by Wilkinson and others (1946), who portray the general distribution of the major geologic units of the area: Paleogene volcanic and sedimentary rocks, Miocene flood basalts of the Columbia River Basalt Group, Miocene and Pliocene basin-fill sediments assigned to the Troutdale Formation, and post-Troutdale unconsolidated deposits. Minor geologic structures were discussed in the accompanying text but not shown on the map. Wilkinson and others (1946) introduced the name Goble Volcanic Series for the thick section of Eocene volcanic and volcaniclastic rocks exposed on both sides of the Columbia River.

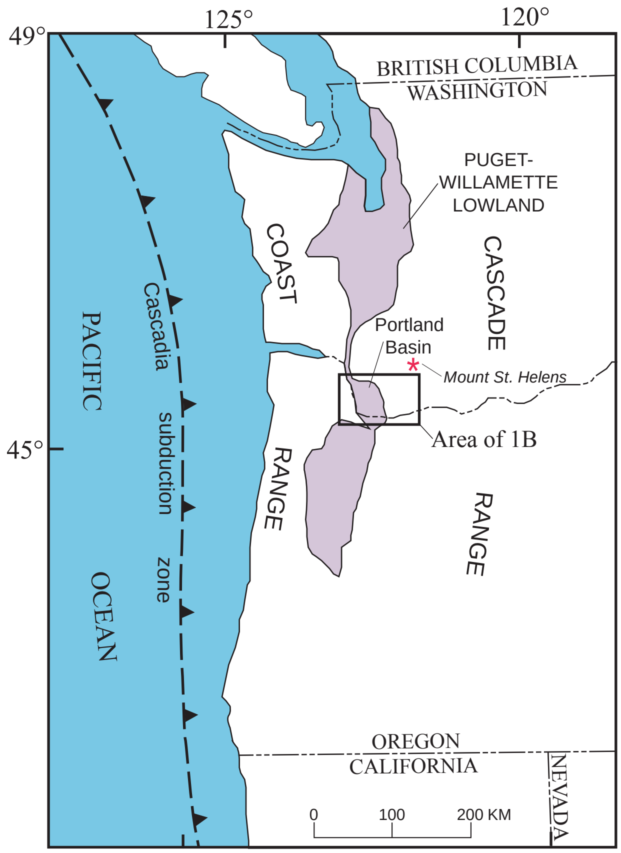


**Figure 1A.** Regional setting of the Woodland quadrangle showing major tectonic and physiographic features of the Pacific Northwest.

The first systematic geologic investigation within the Woodland quadrangle was that of Mundorff (1964), who mapped the area south of the Lewis River to evaluate water resources in Clark County. His 1:48,000-scale map accurately portrays contacts between Tertiary bedrock and the basin-fill units, but he made no attempt to map stratigraphic units within the Tertiary sequence. He proposed a two-fold division of the Troutdale Formation into a lower fine-grained member and an upper coarse-grained member, but did not show the distribution of these members on his map. Mundorff (1964, 1984) described Pleistocene drift and glacier outburst flood deposits in the Lewis River valley but did not distinguish deposits derived from the Quaternary volcanic center of Mount St. Helens.

Swanson and others (1993) updated Mundorff's Clark County work as part of an investigation of ground-water resources throughout the Portland Basin. Their work focused on the basin-fill units, and their map shows hydrogeologic rather than lithostratigraphic units, although there is substantial equivalence between the two. For example, they showed the distribution of a fine-grained confining unit that corresponds to Mundorff's lower member of the Troutdale Formation. They analyzed lithologic logs of 1500 water wells to produce a series of maps that show the elevations and thicknesses of their hydrogeologic units throughout the basin, thus constructing a rough 3-dimensional view of the subsurface stratigraphy of the basin fill.

Phillips (1987a) compiled a geologic map of the Vancouver 30' x 60' quadrangle, which includes the Woodland 7.5' quadrangle, at 1:100,000 scale as part of the state geologic map program of the Washington Division

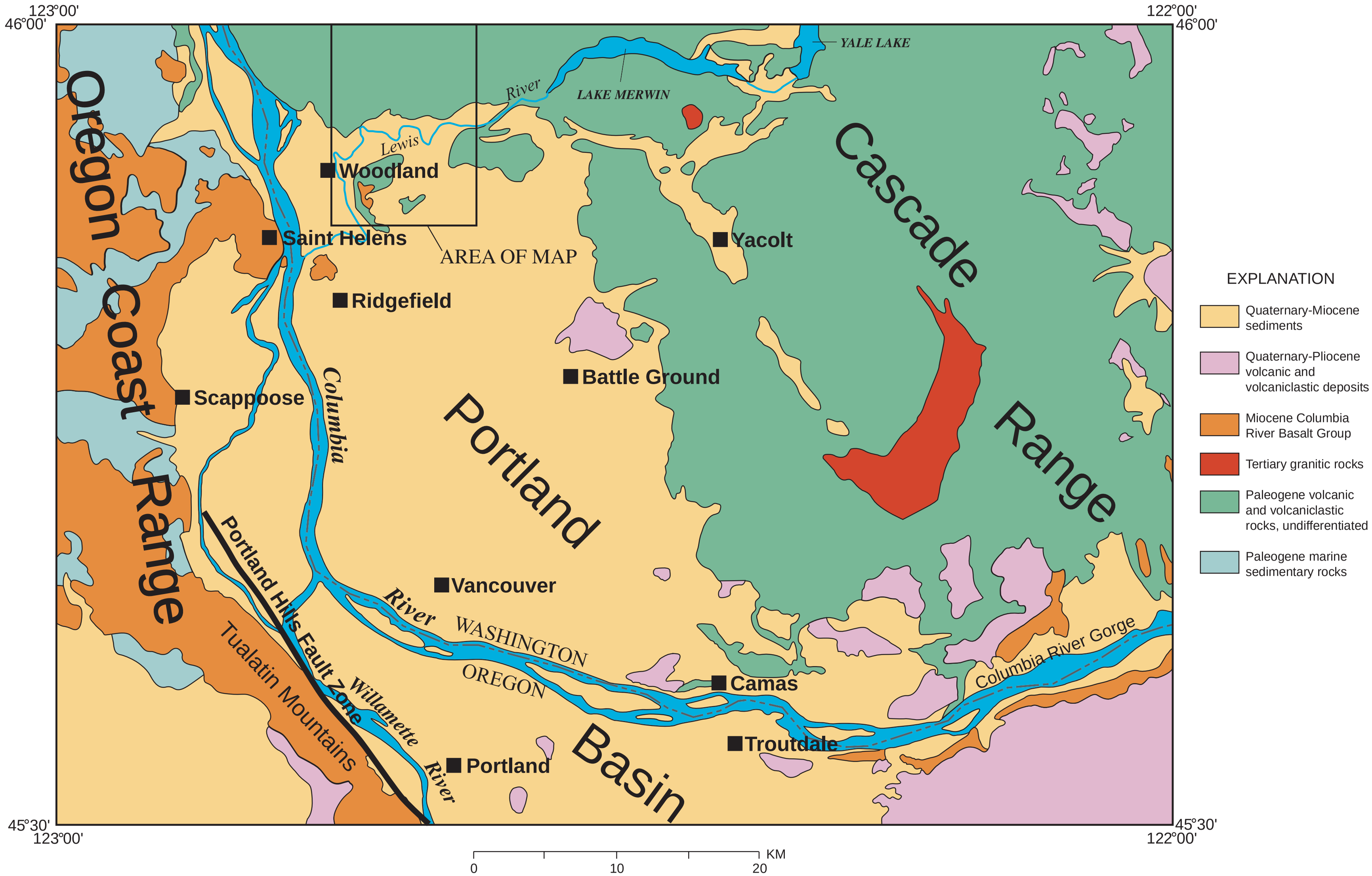


**Figure 1B.** Simplified geologic map of the Vancouver 30' x 60' quadrangle, modified from Phillips (1987a).

of Geology and Earth Resources (Walsh and others, 1987). Although relying heavily on Mundorff's work, he did undertake some original reconnaissance mapping. Phillips was the first to depict Columbia River Basalt Group flows southeast of Woodland and Mount St. Helens-derived volcaniclastic deposits in the lower Lewis River valley. He also mapped informal lithostratigraphic units within the Tertiary bedrock sequence. He acquired chemical analyses for some of the volcanic rocks of the region as well as a few whole-rock K-Ar age determinations.

Several topical investigations have provided additional information on the geology of the Woodland quadrangle and vicinity. Major and Scott (1988) studied the Mount St. Helens-related deposits of the Lewis River valley, which they described but did not map. Fiksdal (1975) and Harp and others (1997) provided data on landslides near Woodland. Mundorff (1984) reported on the glacial deposits of the Lewis River region.


### ACKNOWLEDGMENTS

Access granted by landowners was essential for mapping in the Woodland quadrangle. I thank Robert Ross and Dennis Mohan of the Longview Fibre Company and Ross Graham and Dorothy Yount of Weyerhaeuser Company for permission to work on their timberlands. Kevin Storedahl offered unrestricted access for chemical and paleomagnetic sampling in his quarry south of Woodland. Several U.S. Geological Survey colleagues provided data: David Siems (analytical chemistry), Jonathan Hagstrum (paleomagnetic measurements), Richard Blakely (aeromagnetic maps), Andrei Sarna-Wojcicki (tephrochronology), and Robert Fleck ($^{40}Ar/^{39}Ar$ ages). Chemical analyses at Washington State University were performed by Diane M. Johnson. Kevin Anderson and Bradley Reid gave able field and laboratory assistance in 1997 and 1998, respectively. Sarna-Wojcicki, Kenneth Bishop, Judith Fierstein, and Michael Clynne made available essential laboratory facilities. Debra Hunemuller and Stephanie Abraham of the Washington Department of Ecology Southwest Regional Office in Lacey, Washington provided access to their files of water-well drillers' logs. Connie Manson helped obtain information from the library at the Washington Division of Geology and Earth Resources in Olympia, Washington. I have benefited immensely from discussions on various aspects of the regional stratigraphy, structure, and geologic history of southwestern Washington with Roger Ashley, Marvin Beeson, Michael Clynne, Paul Hammond, Keith Howard, Lee Liberty, Alan Niem, Jim O'Connor, William Phillips, Charles Powell, Stephen Reidel, William Scott, James Smith, Donald Swanson, Mindy Sue Vogel, Karl Wegmann, and Ray Wells. Wegmann shared his unpublished mapping of landslide deposits in Cowlitz County and critiqued an early draft of the manuscript. Marvin Beeson and Brett Cox provided insightful technical reviews.


## SYNOPSIS OF GEOLOGY

The geology of the Woodland quadrangle is dominated by four major groups of deposits: Paleogene bedrock, Miocene lava flows of the Columbia River Basalt Group, Miocene to lower Pleistocene(?) alluvial deposits of the ancestral Columbia River, and Quaternary alluvial and glaciofluvial deposits in the Lewis River valley. Late Eocene volcanic and volcaniclastic rocks and rare small intrusions, early products of the Cascade volcanic arc, underlie the dissected upland north of the Lewis River and are locally exposed beneath younger deposits south of the river. Following mild folding, faulting, and erosion, the bedrock units formed a low-relief terrain within which the Portland Basin began to develop during early Neogene time. Basaltic lavas of the Columbia River Basalt Group and fluvial deposits of the ancestral Columbia River were deposited on the Paleogene bedrock within the subsiding basin. During Pleistocene and Holocene time, alluvial processes in the Lewis River valley have been strongly influenced by regional uplift of the Cascade Range, glaciation in the Cascade Range, eruptive activity at the Mount St. Helens volcanic center, and cataclysmic flooding triggered by the failure of ice dams at glacial Lake Missoula in Montana.

A relatively mild, wet climate prevailed in the western Pacific Northwest throughout most of the Cenozoic era (Wolfe and Hopkins, 1967; Wolfe, 1978). Mountain glaciers formed in the Lewis River valley on several occasions during the Pleistocene (Crandell and Miller, 1974; Mundorff, 1984) but never reached as far downstream as the map area. Long exposure produced saprolitic soil horizons as much as 10 m thick on Paleogene bedrock and Neogene basin-fill deposits. Because of this intense weathering and the dense vegetation of the region, natural outcrops of bedrock are generally limited to steep cliff faces, landslide scarps, and streambeds; most exposures are at roadcuts and quarries. Surface information was supplemented with lithologic data obtained from water-well reports in the files of the Washington Department of Ecology; well locations were taken as described in the reports and were not field checked.

## PALEOGENE BEDROCK

Bedrock in the Woodland quadrangle consists of a diverse assortment of subaerially erupted lava flows and volcaniclastic rocks that are broadly typical of the strata that underlie much of the western slopes of the southern Washington Cascade Range (Evarts and others, 1987; Smith, 1993; Evarts and Swanson, 1994). Bedrock units in the map area generally strike northeast and dip to the southeast at 15° to 30°; deviations from this trend reflect variations in primary dips and subsequent structural disruption. The lower part of the section north of the Lewis River is a heterogeneous assemblage of mafic to silicic lava flows and volcaniclastic strata. Neogene sediments bury much of the stratigraphically higher part of the section south of the river, but where bedrock exposed it is dominated by andesite flows. Dikes, sills, and small plugs that are texturally and compositionally similar to nearby lava flows are concentrated in a east-northeast-trending belt about 3 km wide north of the Lewis River; medium- and coarse-grained dioritic bodies in the vicinity of Houghton Creek are satellitic to an extensive intrusive complex to the east in the adjacent Ariel quadrangle (Evarts, 2004). Attempts to directly date bedrock units in the Woodland quadrangle were unsuccessful, but $^{40}Ar/^{39}Ar$ ages obtained from adjacent areas indicate that the entire bedrock section exposed in the map area is probably late middle to late Eocene, about 39 to 34 Ma (R.J. Fleck, written commun., 2000).

### STRATIGRAPHIC NOMENCLATURE: THE GOBLE PROBLEM

Phillips (1987a) assigned the Eocene rocks of the Woodland quadrangle north of the Lewis River to the Goble Volcanics. The Goble Volcanic Series was named by Wilkinson and others (1946) for volcanic and volcaniclastic rocks exposed near Goble, Oregon, about 10 km northwest of the map area. The name was later revised to Goble Volcanics by Livingston (1966), to conform to the then-current North American Code of Stratigraphic Nomenclature. Included within the Goble Volcanics by Wilkinson and others (1946) are strata in the Deer Island quadrangle (Evarts, 2002) that are contiguous with those in the northern Woodland quadrangle. Wilkinson and others (1946) stated that the formation “extends eastward from the northeast corner of the [Saint Helens 15'] quadrangle to the Lake Merwin area,” about 20 km east of Woodland (fig. 1). In Oregon, the Goble Volcanics is unconformably overlain by micaceous arkosic and tuffaceous sandstones of Oligocene age that were deposited in shallow marine settings.

As discussed by Evarts (2002), the difficulty with employing the Goble Volcanics as a formal lithostratigraphic unit in Washington is that the superjacent marine sedimentary strata do not extend east of the Columbia River. As a result, it is impossible to locate the top of the unit as originally defined, and the lack of a clear lithologic marker that defines its upper contact renders the formation untenable in the southern Washington Cascade Range. Consequently, only informal or lithologic names are used for the volcanic rocks shown on this map.

### LATE EOCENE VOLCANIC AND VOLCANICLASTIC ROCKS

#### Basaltic andesite, basalt, and andesite

The oldest part of the Paleogene section consists predominantly of mafic lava flows and flow breccia of basaltic andesite (Tba) that underlie the mountainous northwestern part of the Woodland quadrangle. Most flows are conspicuously porphyritic, with phenocrysts of plagioclase, olivine, and, in many flows, augite. This flow-dominated section continues to the west and underlies most of the area east of the Columbia River in the adjacent Deer Island quadrangle (Evarts, 2002). A stratigraphically higher sequence of basaltic andesite flows (Thba), distinguished by the presence of hypersthene phenocrysts, crops out on the divide between the Little Kalama and Lewis Rivers in the northeastern part of the map area. Mafic flows are also locally abundant in the intervening, volcaniclastic-dominated, stratigraphic section. Basaltic andesite typically forms blocky to platy jointed flows 3 to 6 m thick that grade into upper and lower flow breccia zones. Abundant zeolite- and clay-filled vesicles and reddish colors, owing to oxidation during cooling, characterize upper flow breccia zones. All flows were apparently emplaced subaerially; no pillow lavas or other indications of subaqueous environments were observed.

Two or more flows of distinctive olivine-phyric basalt (Tob) are intercalated with basaltic andesite flows in the lower Little Kalama River valley. The basalts are distinguished by the presence of conspicuous olivine phenocrysts accompanied by subordinate augite and plagioclase microphenocrysts; the olivine typically contains abundant euhedral inclusions of chromian spinel. The petrography, chemistry, and stratigraphic position of these flows suggest they may be correlative with similar rocks (basaltic andesite of Indian George Creek) mapped by Evarts and Ashley, (1991) in the Lewis River valley to the northeast and with the basalt of Wolf Point of Evarts (2001) in the Silver Lake quadrangle to the north. Regional mapping in the southern Washington Cascade Range (Roberts, 1958; Phillips, 1987a, b; Evarts, 2002; R.C. Evarts, unpub. mapping) shows that the olivine-phyric flows occupy a relatively restricted stratigraphic range in the lower part of the Tertiary section. A whole-rock incremental-heating $^{40}Ar/^{39}Ar$ age of 38.8±0.3 Ma was determined for a basalt of Wolf Point flow south of Silver Lake by R.J. Fleck (oral commun., 1999).

Andesitic lava flows and flow breccias (Ta) are scattered throughout the Paleogene stratigraphic section north of the Lewis River and constitute nearly all of the stratigraphically higher bedrock section to the south. The textures of the flows range from aphyric to moderately porphyritic; all of the porphyritic flows are pyroxene andesites that contain phenocrysts of augite, hypersthene, or both.

### Dacite

Volcanic rocks of silicic composition (Td) are distributed throughout all but the lowest part of the Paleogene stratigraphic section of the Woodland quadrangle. The thickest accumulations of silicic volcanic rocks are at Schumaker Mountain and between Burris and Robinson Creeks about 3 km north of Woodland. Both outcrops appear to be dacitic flow-dome complexes in which the lava flows exhibit complex, partly intrusive contact relations with adjacent clastic rocks. These rocks are typical of Tertiary silicic lavas throughout the southern Washington Cascade Range (Evarts and others, 1987; Evarts and Ashley, 1993) in that they tend to be light colored, platy jointed, flow banded, and sparsely porphyritic. Most flows contain less than 10 percent phenocrysts of plagioclase and pyroxene and lack phenocrysts of hornblende, biotite, or quartz. Although a few silicic lavas retain a glassy (though hydrated) groundmass, most are devitrified or hydrothermally altered to fine-grained assemblages of quartz, feldspar, carbonate, and clay minerals.

### Volcaniclastic rocks

Volcaniclastic rocks make up a substantial proportion of the Paleogene bedrock in the Woodland quadrangle and are divided into: (1) a unit of volcaniclastic sedimentary rocks of predominantly epiclastic origin (Tvs); (2) a tuff unit comprised of mostly pyroclastic rocks (Tt); and (3) a unique basaltic breccia (Tbb) exposed north of Woodland.

Volcaniclastic sedimentary rocks (Tvs) constitute a diverse assemblage of generally well-bedded, texturally and compositionally immature siltstone, sandstone, conglomerate, and breccia. Fragments of volcanic rocks that are petrographically similar to interbedded lava flows are the dominant constituents of most beds; less abundant components include plagioclase, Fe-Ti oxides, and pyroxene crystals, pumice, vitric ash, fine-grained dioritic rocks, and plant remains. Strata of the volcaniclastic sedimentary rocks unit (Tvs) represent a variety of depositional environments and include thin debris-flow and hyperconcentrated flood-flow (Smith, 1986) deposits as well as finer grained fluvial and lacustrine beds probably deposited beyond the flanks of volcanic edifices. In addition to material eroded from older extrusive rocks, many beds in this unit likely contain clasts reworked from unconsolidated penecontemporaneous airfall and ash-flow deposits.

The tuff unit (Tt) consists of andesitic to rhyolitic tuff, pumiceous and lithic lapilli tuff, and lithic tuff breccia that are inferred to be the direct products of explosive eruptions and associated volcanic debris flows. Massive, medium- to coarse-grained, poorly sorted, and matrix supported beds typify this unit. Beds that contain abundant pumice lapilli, originally vitric ash, and carbonized woody debris are interpreted as ignimbrites. Phenocrysts rarely constitute more than 10 percent of juvenile material in the ignimbrites, and include plagioclase, augite, hypersthene, and Fe-Ti oxide, but no quartz, hornblende or biotite. The thickest section of such pyroclastic rocks crops out in the vicinity of Butte Hill; at least 150 m of massive pumiceous tuff and lapilli tuff are well exposed in Robinson and Ross Creeks. In the valley of Burris Creek to the west, these tuffaceous rocks interfinger with basaltic andesite flows. In the northeast part of the map area, several thinner sequences of tuffaceous strata are complexly interbedded with sedimentary rocks and lava flows. Commonly interbedded with the ignimbrites are diamictites that contain angular clasts of volcanic rock as large as 5 m across in a tuffaceous matrix; these beds are inferred to be of lahar or block-and-ash-flow origin.

A massive, unsorted, monolithologic breccia (Tbb) composed of angular clasts as large as 1 m across of seriate basaltic andesite crops out on a south-facing slope at the edge of the quadrangle about 2.5 km north of Woodland. The texture of the deposit is strikingly similar to that of the 1980 debris-avalanche deposit at Mount St. Helens, but it is more indurated. Wilkinson and others (1946) mapped this deposit as a volcanic breccia bed within the Troutdale Formation and interpreted it as recording contemporaneous Pliocene volcanism. However, the clasts petrographically resemble some Eocene basaltic andesite flows that crop out to the east, and a plagioclase $^{40}Ar/^{39}Ar$ age of 37.3±0.3 Ma was obtained for a sample collected in the adjacent Deer Island quadrangle (Evarts, 2002). Although the bed could be a Neogene landslide deposit, I interpret it as Eocene bedrock because of its indurated nature and the apparent absence of similar deposits in Neogene sedimentary units elsewhere in the northern Portland Basin, which indicates that the Cascade Range at this time lacked the high relief necessary to generate a debris avalanche.

## INTRUSIVE ROCKS

Dikes, sills, and small plugs ranging in composition from basalt to andesite are scattered throughout the quadrangle but are most abundant in an eastward-widening swarm north of the Lewis River, where subvertical to steeply north-dipping dikes, typically 1 to 3 m wide, strike preferentially N. 75° E., parallel to the overall trend of the swarm. Dikes and thin sills are undoubtedly more common than portrayed on the map, but many are undetected owing to the limited bedrock exposures. Most exhibit aphyric and porphyritic textures similar to those of the extrusive rocks, and some probably occupy subvolcanic vents of the nearby flows and thus are not much younger than their late Eocene host rocks. Other dikes are somewhat coarser grained, and tend to be more altered than their host rocks. At one locality in Robinson Creek, an altered microdiorite dike cuts through a less altered dike of basaltic andesite, so the coarser grained intrusions may be somewhat younger than the finer grained (but compositionally similar) ones.

A few larger intrusions of fine- to medium-grained, seriate to hypidiomorphic granular, pyroxene diorite also crop out within the intrusive belt. They generally display more pervasive hydrothermal alteration than the smaller bodies, and are flanked by thin contact-metamorphic zones. Near Houghton Creek, dioritic and quartz dioritic intrusions mark the western fringe of a concentration of intrusions centered in the adjacent Ariel quadrangle. Abundant epidote and calcite veins in the volcanic rocks directly north of Clover Valley suggest another intrusion is present at shallow depth there. The ages of the diorites are unknown, but the relatively coarse grain size indicates emplacement depths of hundreds of meters, which suggests crystallization occurred well after deposition of their late Eocene host rocks. Regional relations (Evarts and Swanson, 1994) indicate it is unlikely that any of the intrusions are younger than early Miocene. Intrusion sometime during the Oligocene seems most probable.

## ROCK CHEMISTRY

In general, the chemistry of Paleogene lava flows and intrusive rocks in the Woodland quadrangle (table 1) resembles that of Tertiary igneous rocks sampled elsewhere in the southern Washington Cascade Range (Evarts and Ashley, 1990a,b, 1991, 1992; Evarts and Bishop, 1994; Evarts and Swanson, 1994; Evarts, 2001, 2002; R.C. Evarts, unpub. data). The compositions of igneous rocks in the quadrangle range from basalt to rhyolite (fig. 2A), forming a low- to medium-potassium suite (fig. 2B; the extremely low $K_2O$ and $Na_2O$ concentrations in the rhyolite sample probably reflect loss of alkalies during hydration of original glass; for example, Cerling and others (1985)). Rock compositions straddle the dividing line between tholeiitic and calc-alkaline compositions using the classification of Miyashiro (1974; fig. 2C) and display the low $TiO_2$ (fig. 2D) contents that typify volcanic arc magmas (Gill, 1981). The olivine-phyric basalt flows (Tob) are distinguished by MgO contents greater than 8 wt percent (fig. 2D), and generally exhibit chemical characteristics similar to the basalt of Wolf Point of Evarts (2001).

## METAMORPHISM AND HYDROTHERMAL ALTERATION

Paleogene rocks in the Woodland quadrangle have been subjected to zeolite-facies regional metamorphism, the general character of which is similar to that described from other areas in the southern Washington Cascade Range (Fiske and others, 1963; Wise, 1970; Evarts and others, 1987; Evarts and Swanson, 1994). This region-wide metamorphism reflects burial of the late Eocene rocks by younger volcanics within the relatively high-heat-flow environment of an active volcanic arc. Neither the grade of metamorphism nor the intensity of recrystallization increase perceptively with stratigraphic depth within the quadrangle.

The extent of replacement of igneous minerals by secondary phases ranges from incipient to complete. Permeable, glass-rich, silicic volcaniclastic rocks are the most susceptible to zeolitization, whereas massive lava flows may be only slightly affected. The primary effect of very-low-grade metamorphism in mafic to intermediate-

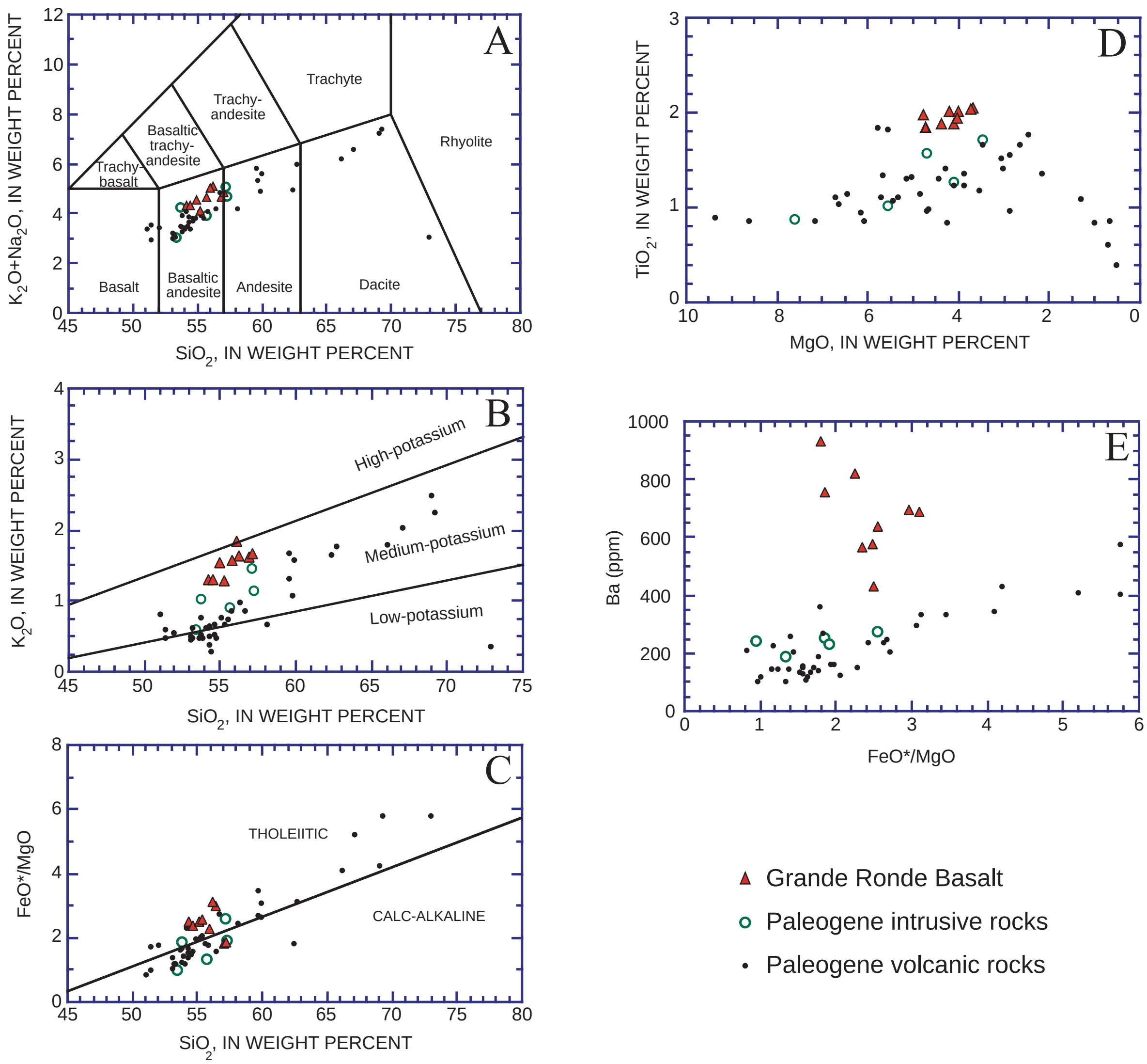


**Figure 2.** Chemical characteristics of volcanic rocks from the Woodland 7.5' quadrangle (analyses recalculated volatile-free). *A*, $K_2O+Na_2O$ versus $SiO_2$, showing IUGS classification (Le Maitre, 2002); *B*, $K_2O$ versus $SiO_2$, showing low-, medium-, and high-potassium fields extrapolated from Gill (1981, p. 6); *C*, FeO*/MgO versus $SiO_2$, showing classification into tholeiitic and calc-alkaline rocks according to Miyashiro (1974), *D*, $TiO_2$ versus MgO; *E*, Ba versus FeO*/MgO. FeO*, total Fe as FeO.

composition lava flows is the development of clay minerals and zeolites that replace labile interstitial glass, fill vesicles, and are deposited on joint surfaces. Feldspar typically displays partial alteration along fractures and cleavage planes to clay minerals and (or) zeolites. Olivine phenocrysts in most basalts and basaltic andesites are totally replaced by smectite with or without hematite and calcite; however, replacement is incomplete in olivine-rich flows. Primary augite and Fe-Ti oxides are largely unaffected by the zeolite-facies metamorphism. Hypersthene phenocrysts in pyroxene andesite flows commonly exhibit minor replacement by dark brown smectite. Alteration tends to be more pervasive in the volcaniclastic rocks and flow breccias. Smectitic clay minerals and zeolites pseudomorphically replace framework grains and fill pore spaces; the development of iron-rich smectites gives these rocks their characteristic green colors. The widespread presence of heulandite and clinoptilolite in pyroclastic rocks of the map area indicates that, except for areas near intrusions, metamorphic temperatures did not exceed 180°C (Cho and others, 1987). Many thick silicic flows and domes exhibit pervasive devitrification and alteration to cryptocrystalline quartz, feldspar, kaolinite, calcite, and hematite. Alteration of this type is common in Tertiary silicic lavas in the Cascade Range (Evarts and others, 1987) because the viscous flows accumulate near source vents where they are exposed to postcrystallization fumerolic activity.

In the eastern part of the Woodland quadrangle, volcanic rocks adjacent to dioritic intrusions are recrystallized to fine-grained assemblages characterized by epidote, chlorite, calcite, and pyrite. The contact-metamorphic minerals occur as replacements of igneous phases and as fracture fillings. Such epidote-bearing hornfels, commonly referred to as propylitic alteration, is widely developed in the contact aureoles of the large Miocene plutons in the Washington Cascade Range (Grant, 1969; Evarts and others, 1987). In the map area, the propylitized zones are fringed by a broad area, extending from Butte Hill to the east edge of the quadrangle, in which secondary calcite is widely distributed as veins and replacements in the volcanic rocks. The general spatial association of carbonate with intrusive rocks indicates that the $CO_2$ was introduced by devolatilization of crystallizing intrusions. Sporadically distributed within the calcite-bearing fringe are patches of more intense metasomatic hydrothermal alteration in which primary feldspar and pyroxene minerals are largely to totally replaced by some combination of albite, calcite, chlorite, epidote, montmorillonite, kaolinite, zeolite, quartz, titanite, and pyrite. Supergene alteration has converted some of these metasomatic rocks to bleached limonitic rocks composed of kaolinite, carbonates, and goethite. The metasomatic hydrothermal alteration is attributed to reactions with low-temperature hydrothermal fluids generated from cooling intrusions at depth and circulated widely through the upper crust along permeable structural zones; therefore, the presence of such alteration provides an important clue for inferring the existence of faults within the poorly exposed Paleogene section.

## NEOGENE FILL OF THE PORTLAND BASIN

The Portland Basin is a structural depression floored by late Eocene and Oligocene rocks and filled with Neogene deposits. As described in previous studies, most of the fill comprises three stratigraphic units: the Columbia River Basalt Group, the Sandy River Mudstone, and the Troutdale Formation (Trimble, 1963; Mundorff, 1964; Swanson and others, 1993). This map is generally consistent with the earlier work but suggests some refinements of stratigraphic relations and age assignments.

### COLUMBIA RIVER BASALT GROUP

In Miocene time, between 16.5 and 6 Ma, huge volumes of tholeiitic flood basalt erupted from fissures in southeastern Washington and adjacent areas of Oregon and Idaho, forming the Columbia River Basalt Group. Some of the largest flows moved westward through a broad lowland across the Cascade Range and ultimately reached the Pacific Ocean (Snavely and others, 1973; Tolan and others, 1989; Wells and others, 1989). West of the Cascade Range, thick flows buried large areas of a low-relief Coast Range terrane (Beeson and others, 1989). Dissected remnants now blanket upland areas west of the Columbia River (Wilkinson and others, 1946; Evarts, 2002). The most voluminous formation of the Columbia River Basalt Group is the Grande Ronde Basalt (Tolan and others, 1989), which erupted during a one-million-year span beginning at 16.5 Ma; all of the Neogene basalt flows exposed in the Woodland quadrangle belong to the Grande Ronde. Based on chemical and paleomagnetic data, some of the small flow remnants attached to the valley wall southeast of Woodland correlate with outcrops in the Deer Island quadrangle to the west, indicating that the flows once extended across the Columbia River valley. Grande Ronde Basalt flows are distinguished from other Columbia River Basalt Group formations by their relatively low $TiO_2$ contents (Swanson and others, 1979; Mangan and others, 1986; Beeson and others, 1989; Reidel and others, 1989; Hooper, 2000) and they are readily distinguished from Paleogene volcanic rocks by their distinctive, glass-rich, intersertal and microvesicular texture, lack of alteration and their chemical composition (table 1). Although both the Miocene and Eocene flows are chiefly basaltic andesites (fig. 2A), all of the Grande Ronde Basalt flows are tholeiites (fig. 2C) that contain less $Al_2O_3$ and more FeO*, $TiO_2$, and $K_2O$ than the Eocene flows, and have a more

| Geologic age | | Group | | Formation | Series | Age (Ma) | Magnetic Polarity |
|---|---|---|---|---|---|---|---|
| Miocene | Late | Columbia River Basalt Group | Yakima Basalt Subgroup of Swanson and others (1979) | Saddle Mountains Basalt | **Lower Monumental Member** | 6 | N |
| | | | | | *Erosional Unconformity* | | |
| | | | | | **Ice Harbor Member** | 8.5 | |
| | | | | | Basalt of Goose Island | | N |
| | | | | | Basalt of Martindale | | R |
| | | | | | Basalt of Basin City | | N |
| | | | | | *Erosional Unconformity* | | |
| | | | | | **Buford Member** | | |
| | Middle | | | | **Elephant Mountain Member** | 10.5 | N, T |
| | | | | | *Erosional Unconformity* | | |
| | | | | | **Pomona Member** | 12 | R |
| | | | | | *Erosional Unconformity* | | |
| | | | | | **Esquatzel Member** | | N |
| | | | | | *Erosional Unconformity* | | |
| | | | | | **Weissenfels Ridge Member** | | |
| | | | | | Basalt of Slippery Creek | | N |
| | | | | | Basalt of Tenmile Creek | | N |
| | | | | | Basalt of Lewiston Orchards | | N |
| | | | | | Basalt of Cloverland | | N |
| | | | | | **Asotin Member** | 13 | |
| | | | | | Basalt of Huntzinger | | N |
| | | | | | *Local Erosional Unconformity* | | |
| | | | | | **Wilbur Creek Member** | | |
| | | | | | Basalt of Lapwai | | N |
| | | | | | Basalt of Wahluke | | N |
| | | | | | *Local Erosional Unconformity* | | |
| | | | | | **Umatilla Member** | | |
| | | | | | Basalt of Sillusi | | N |
| | | | | | Basalt of Umatilla | | N |
| | | | | | *Local Erosional Unconformity* | | |
| | | | | Wanapum Basalt | **Priest Rapids Member** | 14.5 | |
| | | | | | Basalt of Lolo | | R |
| | | | | | Basalt of Rosalia | | R |
| | | | | | *Local Erosional Unconformity* | | |
| | | | | | **Roza Member** | | T, R |
| | | | | | **Frenchman Springs Member** | | |
| | | | | | Basalt of Lyons Ferry | | N |
| | | | | | Basalt of Sentinel Gap | | N |
| | | | | | Basalt of Sand Hollow | 15.3 | N |
| | | | | | Basalt of Silver Falls | | N, E |
| | | | | | Basalt of Ginkgo | 15.6 | E |
| | | | | | Basalt of Palouse Falls | | E |
| | | | | | **Eckler Mountain Member** | | |
| | | | | | Basalt of Shumaker Creek | | N |
| | | | | | Basalt of Dodge | | N |
| | | | | | Basalt of Robinette Mountain | | N |
| | | | | | *Local Erosional Unconformity* | | |
| | | | | Grande Ronde Basalt | ***Member of Sentinel Bluffs*** | 15.6 | $N_2$ |
| | | | | | **Member of Slack Canyon** | | |
| | | | | | **Member of Fields Spring** | | |
| | | | | | ***Member of Winter Water*** | | |
| | Early | | | | **Member of Umtanum** | | |
| | | | | | **Member of Ortley** | | |
| | | | | | **Member of Armstrong Canyon** | | |
| | | | | | **Member of Meyer Ridge** | | $R_2$ |
| | | | | | ***Member of Grouse Creek*** | | |
| | | | | | **Member of Wapshilla Ridge** | | |
| | | | | | **Member of Mt. Horrible** | | |
| | | | | | **Member of China Creek** | | $N_1$ |
| | | | | | **Member of Downy Gulch** | | |
| | | | | | **Member of Center Creek** | | $R_1$ |
| | | | | | **Member of Rogersburg** | | |
| | | | | | **Teepee Butte Member** | | |
| | | | | | **Member of Buckhorn Springs** | 16.5 | |
| | | | | Imnaha Basalt | | | $R_1$ |
| | | | | | | | T |
| | | | | | | | $N_0$ |
| | | | | | | 17.5 | $R_0$ |

**Figure 3.** Stratigraphic nomenclature of the Columbia River Basalt Group and related units, after Tolan and others (1989). Terminology for informal members of the Grande Ronde Basalt described by Reidel and others (1989) is that of Reidel (1998). Magnetic polarity designations are N, normal; R, reversed; T, transitional; E, excursional; subscripts refer to magnetostratigraphic units of Swanson and others (1979). Time scale of Berggren and others (1995). Units present in the Woodland 7.5' quadrangle are shown in bold italics.

restricted range of MgO contents (figs. 2B, D). Trace-element contents, particularly Ba, also serve to differentiate between the Grande Ronde Basalt and the Paleogene volcanic rocks (fig. 2E).

On the basis of lithologic, chemical and paleomagnetic criteria, Reidel and others (1989) divided the Grande Ronde Basalt in the Columbia Basin into several informal members (fig. 3), which they called units but were later referred to as members by Reidel (1998). Beeson and others (1989) and Wells and others (1989) traced several of these members into the Portland Basin and westward into the Coast Range. Chemical and paleomagnetic properties of the Grande Ronde flows in the Woodland quadrangle were used to correlate them with the informal members of Reidel (1998). [1]

The youngest informal member in the map area (Tgsb) consists of normally magnetized, high-MgO (4.3 to 4.7 wt percent; table 1, nos. 52-54; table 2) basalt correlated with the member of Sentinel Bluffs, the youngest member of the Grande Ronde Basalt in the Columbia Basin. Two flows or flow groups can be distinguished using data from this and adjacent quadrangles: the older is characterized by microphyric textures and relatively low $TiO_2$ contents (1.81-1.90 wt percent), the younger is characterized by aphyric to very sparsely microphyric textures and higher $TiO_2$ contents (1.94-2.02 wt percent). The lower part of a relatively high-$TiO_2$ Sentinel Bluffs flow is exposed in a small, abandoned quarry 2 km east-southeast of Woodland. This flow consists of blocky-columnar-jointed diktytaxitic basalt that contains widely dispersed plagioclase phenocrysts. In 1998, prior to reclamation of the quarry, the base of the flow was exposed, resting directly on thin, subhorizontal beds of carbonaceous, clayey, sedimentary rocks (Tsr).

Another flow (Tgww), also normally magnetized, underlies the slope below and west of the Sentinel Bluffs flows. This flow has a relatively low MgO content (3.6 to 3.7 wt percent; table 1, nos. 50-51; table 2) and is assigned to the member of Winter Water (Winter Water unit of Reidel and others, 1989). Prior to reclamation in 1998, excellent quarry-wall exposures of the Winter Water flow revealed a 30-m-thick entablature abruptly overlying a well-developed colonnade. The base of the flow was not exposed, but in the east wall of the quarry the massive flow graded into pillow basalt banked against a section of clayey sedimentary rocks (Tsr), representing a preserved segment of the wall of the canyon filled by the flow. In one location, a finger of basalt extended into and deformed the sedimentary beds, an example of the invasive relations that are widely exhibited by Grande Ronde Basalt flows (Byerly and Swanson, 1987; Tolan and Beeson, 1999; Wells and Niem 1987).

A third type of Grande Ronde Basalt flow (Tggc(?)) in the Woodland quadrangle is characterized by intermediate MgO contents (3.9-4.0 wt percent; table 1, nos. 46-49) and reversed remnant magnetic polarity. This flow crops out in a large quarry about 2.5 km southeast of Woodland, where it is unconformably overlain by as much as 15 m of Troutdale Formation conglomerate. Quarry walls reveal roughly 50 m of hackly fractured basalt divided into three zones by two gently dipping, highly vesicular horizons, each less than 1 m thick. The chemical compositions of the nonvesicular zones are virtually identical, thus they are probably lobes of a single flow. Quarry-floor exposures show that the basalt overlies and locally invades beds of claystone and hyaloclastite (Tsr and Tbh). A similar relation was observed in a small stream valley 2.5 km east-southeast of Woodland. The identity of this flow is uncertain because its chemistry does not precisely match published data for any Grande Ronde Basalt flow, displaying lower FeO* and higher CaO and Cr contents than most (Reidel and others, 1989; Beeson and others, 1989; Mangan and others, 1986). It most closely matches a reversely magnetized flow that lies stratigraphically between the members of Whapshilla Ridge and Ortley on the west side of the Columbia Basin (S.P. Reidel, written, commun., 2004), so is tentatively assigned to the member of Grouse Creek (fig. 3). The relative topographic positions of the Grande Ronde Basalt members near Woodland indicate there was a period of fluvial incision between emplacement of the Grouse Creek(?) flow and the younger flows of the members of Winter Water and Sentinel Bluffs.

In the valley of a small tributary of the Lewis River southeast of Woodland, the member of Grouse Creek(?) rests on a section of distinctive, coarse-grained, yellow to brown, basaltic sedimentary rocks (Tbh). The deposit forms a lensoidal body as thick as 25 m that evidently fills a small valley cut into the underlying Sandy River Mudstone (Tsr). The unit consists of poorly sorted, massively bedded, clast-supported conglomerate with a

[1] Comparison of chemical analyses obtained for this report with older data in the literature (Reidel and others, 1989; Beeson and others, 1989), all of which were performed in the same laboratory at Washington State University, suggested that systematic biases were present. Re-analysis of a suite of 38 Columbia River Basalt Group samples, originally analyzed in 1983, confirmed this suspicion. The reasons for the discrepancies are unclear but probably relate to a change in instrumentation in the laboratory in 1986 (D.M. Johnson, written commun., 2001). Among the elements most useful in discriminating between Grande Ronde Basalt flows, the newer data exhibit consistently higher contents of $TiO_2$ (3.5%) and $P_2O_5$ (8.0%) and lower MgO (2.5%)(percentages are average relative differences between the datasets). These differences were taken into account in evaluating the data for correlation purposes.

sandy matrix of partly palagonitized basaltic glass; associated sandstone beds are similar to the conglomerate matrix. Most pebbles and cobbles in the conglomerate are moderately to well rounded and nearly all consist of Grande Ronde Basalt; a few are angular and possess glassy rinds, resembling pillow fragments. Some of the conglomeratic beds resemble those of the Troutdale Formation but lack the exotic quartzite, granitic, and Cascadian volcanic clasts that characterize the Troutdale. The petrography and chemistry of the sandstone (table 1, no. 45) indicate that it, like the larger clasts, also is derived from Grande Ronde Basalt. Angular claystone boulders as large as 1 m across, presumably ripped up from the subjacent strata, are dispersed through the lower part of the deposit. The deposit is interpreted as the product of mixing between fluvial channel gravels and hyaloclastic debris generated by explosive basalt-water interactions during emplacement of the overlying Grande Ronde Basalt flow. Vague bedding dips eastward at a low angle; this and the restricted distribution of the deposit suggest the water involved was supplied by a tributary stream rather than the ancestral Columbia River. Smith (1988) described similar hyaloclastites and pillow lavas associated with Grande Ronde flows along the western margin of the Columbia Basin. He attributed them to the explosive interaction of lava with the water of transient lakes impounded where the flows blocked streams. Similarly, Beeson and others (1985) noted that the development of hyaloclastites associated with Columbia River Basalt Group flows in western Oregon seems to be restricted to flow margins near the mouths of pre-existing tributary streams.

## SANDY RIVER MUDSTONE AND TROUTDALE FORMATION

As the Portland Basin continued to subside during the late Miocene and Pliocene, it filled with continental fluvial and lacustrine sediments that were transported through the Cascade Range by the ancestral Columbia River as well as with locally derived detritus carried in by tributaries draining the surrounding highlands. These deposits have been mapped from the Columbia River Gorge west and north along the Columbia River to Kelso, Washington, about 15 km north of the map area (Wilkinson and others, 1946; Lowry and Baldwin, 1952; Livingston, 1966; Trimble, 1957, 1963; Mundorff, 1964; Tolan and Beeson, 1984; Phillips, 1987a, b). Most workers assigned these nonmarine sedimentary beds to the Troutdale Formation of Hodge (1938). In its type area near the west end of the Columbia River Gorge, the Troutdale Formation is composed of three characteristic sedimentary rock types: basalt-clast conglomerate, arkosic sandstone, and basaltic vitric sandstone. The conglomerate consists chiefly of well-rounded pebbles and cobbles eroded from flows of the Columbia River Basalt Group, but its most distinctive components are well-rounded, light-colored but commonly iron-stained pebbles of quartzite, granite, and foliated metamorphic rocks. These rock types are foreign to western Oregon and Washington and must have been transported by the ancestral Columbia River from terranes composed of pre-Tertiary granitic and metamorphic rocks in northeastern Washington, Idaho, and British Columbia. The arkosic sandstone consists largely of quartz, plagioclase, potassium feldspar, and felsic rock fragments and contains minor but conspicuous muscovite and biotite. Its composition, like that of the conglomerate, points to source terranes east of the Cascade Range. The vitric sandstone consists of poorly sorted, relatively coarse-grained, variably palagonitized hyaloclastic debris. The petrography and chemistry of the vitric clasts resemble those of olivine-bearing, high-alumina basalt and basaltic andesite flows erupted from volcanic centers flanking the Columbia River in the Cascade Range during Pliocene time (Tolan and Beeson, 1984; Swanson, 1986). Near the margins of the Portland Basin, the Troutdale Formation contains debris eroded from adjacent volcanic highlands. Tolan and Beeson (1984) refer to these locally derived deposits as the Cascadian stream facies of the Troutdale Formation, which they distinguish from the more typical ancestral Columbia River facies.

Scattered outcrops and abundant subsurface data from water-well drillers' logs show that, in much of the Portland Basin, a conglomeratic section as much as 120 m thick overlies a sequence of finer grained strata. This observation prompted Trimble (1957) and Mundorff (1964) to divide the Troutdale Formation into informal upper and lower members based on the pronounced difference in grain size. Trimble (1963) later formally named the lower, fine-grained member the Sandy River Mudstone.

More recently, Howard (2002) mapped the Battle Ground quadrangle to the southeast of the Woodland quadrangle and employed lithologic and geomorphic criteria to subdivide Mundorff's (1964) Troutdale Formation. Following Mundorff (1964), Howard (2002) assigned most of the conglomerate that underlies the terrain north of the East Fork Lewis River to the Troutdale Formation. However, he noted that coarse-grained deposits found at lower elevations along and south of the East Fork, also mapped as Troutdale Formation by Mundorff, are younger and were derived primarily from the adjacent Cascade Range rather than from the Columbia River Basin. Howard

(2002) mapped these deposits as an informal alluvial-fan member of the Troutdale Formation, which he suggested may include early Pleistocene outwash.

On this map, Neogene sedimentary deposits that were previously assigned to the Troutdale Formation (Mundorff, 1964; Phillips, 1987a) are divided into three units based on lithology and stratigraphic position. These units generally correspond to those distinguished by Howard (2002), although the names and some interpretations regarding correlations and ages differ (fig. 4). The relatively fine-grained sedimentary rocks, equivalent to the informal lower member of the Troutdale Formation of Mundorff (1964) and the informal fine-grained member of the Troutdale Formation of Howard (2002) are here assigned to the Sandy River Mudstone (unit Tsr). As recognized by Howard (2002), coarse-grained sedimentary rocks that overlie the Sandy River Mudstone in the map area comprise deposits of two ages separated by an erosional unconformity. The older conglomeratic deposits underlie a dissected, gently south- to southwestward-sloping terrain south of the Lewis River that Mundorff (1964) called the

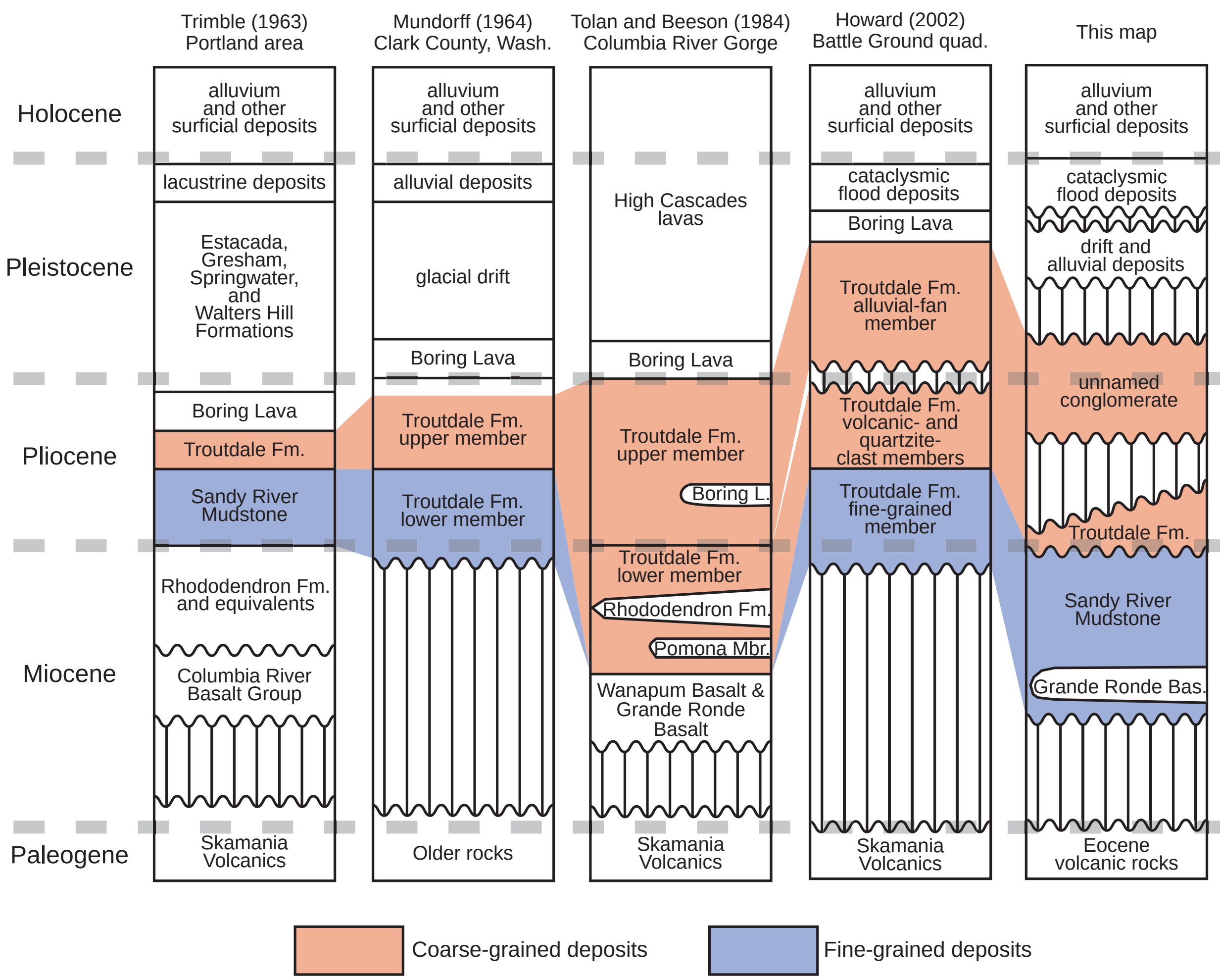


**Figure 4.** Comparison of stratigraphic nomenclature and age assignments for Neogene basin-fill units of the Portland Basin and vicinity.

Troutdale bench. These deposits disconformably overlie the Sandy River Mudstone and are herein assigned to the Troutdale Formation. They are stratigraphically and lithologically equivalent to Howard's (2002) informal quartzite-clast and volcanic-clast members of the Troutdale Formation. The younger unnamed conglomerate (QTc) crops out at lower elevations near the southern edge of the Woodland quadrangle and is inset against the Sandy River Mudstone and Troutdale Formation; it is equivalent to Howard's (2002) informal alluvial-fan member of the Troutdale Formation.

Surface data and numerous water-well logs indicate that the basin fill buries an eroded bedrock surface of considerable relief. The bedrock-altitude map of Swanson and others (1993) shows a pronounced northwest-trending paleovalley between Pine Grove and Highland filled with as much as 250 m of Neogene sediments. The slope of the surface of the Troutdale bench projects northward across the Lewis River and intersects the north valley wall at an elevation of roughly 1000 ft (300 m). The existence of several patches of Columbia River Basalt-cobble conglomerate along the north valley wall, including one at 900 ft (275 m) near the east boundary of the map area, confirms that Neogene sediments lapped onto Paleogene bedrock in that area, and were subsequently stripped by downcutting of the Lewis River.

Sandy River Mudstone (Tsr) is exposed in small stream valleys near the south boundary of the map area, roadcuts on the south side of the Lewis River valley, and quarries along the Columbia River valley wall southeast of Woodland. Soft, subhorizontally bedded sedimentary strata that locally crop out in the banks of the Lewis River at and upstream from the mouth of Houghton Creek probably also belong to this formation. Water-well drillers' logs indicate the unit underlies the Troutdale Formation (Ttf) throughout the area south of the Lewis River, where it may be 240 m thick (Mundorff, 1964; Swanson and others, 1993). It consists of well-bedded claystone, siltstone, and sandstone, with minor interbeds of pebbly conglomerate, pumice-lapilli tuff, and lignite. Most of the sandy beds are micaceous lithic and arkosic sandstones that are bluish gray in fresh exposures but rapidly oxidize to light brown or tan; some are thoroughly cemented by limonite. Claystone beds are commonly carbonaceous and locally contain well-preserved leaf impressions. Many are tuffaceous and contain thoroughly weathered tephra that was presumably derived from the nearby volcanic arc. Claystone increases in abundance downsection. Sedimentary structures indicate a fluvial depositional setting (Miall, 1977, 1996): the sandstones exhibit graded bedding, planar and trough cross-beds, and cut and fill structures indicative of channel facies, whereas the carbonaceous claystones are interpreted as overbank deposits.

Southeast of Woodland, claystone-dominated strata clearly underlie the Grande Ronde Basalt flows, which no doubt accounts for their preservation. Steep claystone-basalt contacts suggest the lava flows occupy channels incised into the subjacent sediments. Locally, small fingers of lava invade and deform the claystone, showing that the sediments were unconsolidated and probably water saturated when overrun by the basalt. This suggests that little time elapsed between their deposition and the emplacement of the Grande Ronde flows.

The Troutdale Formation (Ttf) consists largely of cobbly conglomerate, which drillers' logs show is as much as 70 m thick. Intense weathering to depths exceeding 30 m has converted much of it into red-brown clayey soil with no vestige of its original character except for a local lag of residual quartzite pebbles (Mundorff, 1964; Swanson and others, 1993). The best exposure of the unit in the map area is in the highwall of a quarry about 2.5 km southeast of Woodland, where approximately 15 m of weakly cemented conglomerate rests unconformably on deeply weathered Grande Ronde Basalt. Below a 5-m-thick red soil horizon are massive beds of openwork and sandstone-matrix pebble and cobble conglomerate and rare thin lenses of basaltic sandstone and grit. Nearly all clasts are well rounded. Most are virtually aphyric basalts of the Columbia River Basalt Group; the remainder includes light-colored granitic and quartzofeldspathic metamorphic rocks, Fe-oxide stained quartzite, and rare but conspicuous clasts of light-gray weathering pyroxene andesite that is lithologically similar to those in lahar breccias of the late Miocene Rhododendron Formation in the Columbia River Gorge (Tolan and Beeson, 1984). Most of these components, like those of the conglomeratic and sandy beds in the Sandy River Mudstone, must have been transported into the map area by an ancestral Columbia River. The conglomerate mapped as Troutdale Formation about 3 km north of Woodland contains abundant clasts of Tertiary volcanic rocks derived from the Cascade Range as well as clasts of the Columbia River Basalt Group, documenting a mixed Columbia River-Lewis River source in that area. Sedimentologic characteristics of the conglomerate, such as the massive to crudely stratified beds, clast-support, openwork and sand-matrix textures, moderate to good sorting, and clast imbrication, are consistent with deposition during flood stage in a shallow gravelly braided river system (Miall, 1977, 1996; Rust, 1978; Ramos and Sopeña, 1983).

The basal contact of the Troutdale Formation with the Sandy River Mudstone is a disconformity. In outcrop, Troutdale Formation conglomerate commonly occupies small channels cut into concordant fine-grained beds of the Sandy River Mudstone. Well data indicate relatively little relief, perhaps 100 ft or less, on the surface of the Sandy River Mudstone. The amount of time represented by the erosional unconformity is unknown.

No dateable beds were found in the Sandy River Mudstone and Troutdale Formation of the Woodland quadrangle. Wilkinson and others (1946) recovered late Miocene or early Pliocene fossil leaves from fine-grained strata about 3 km northwest of Woodland that, although not contiguous with Neogene sediments south of the Lewis River, are lithologically similar to the Sandy River Mudstone (Mundorff, 1964; Evarts, 2002). Fossil floras collected from the Sandy River Mudstone of northern Oregon were assigned an early Pliocene age (Trimble, 1963). In all these localities, the fossils were obtained from horizons interpreted to be near the top of the unit (Trimble, 1963; Mundorff, 1964). In the few places where the base of the Sandy River Mudstone is exposed along the edge of the Portland Basin, it rests unconformably on rocks ranging in age from late Eocene to late Miocene, and the formation has conventionally been considered to postdate the Columbia River Basalt Group (Trimble, 1963; Swanson and others, 1993). Near Woodland, however, strata lithologically indistinguishable from the Sandy River Mudstone overlie and are invaded by both normally and reversely magnetized flows of the Grande Ronde Basalt, demonstrating that the lowest part of the formation is considerably older than previously inferred. Lithologically similar stratigraphic units that are probably in part coeval with the Sandy River Mudstone of the Woodland quadrangle include the lower part of the Ellensburg Formation in the Columbia Basin, the upper parts of the Scotts Mills and Molalla Formations in the Willamette valley, and the Astoria Formation and correlative strata in the Coast Range to the west, all of which locally exhibit invasive relations with flows of the Grande Ronde Basalt (Van Atta and Kelty, 1985; Byerly and Swanson, 1987; Wells and Niem 1987; Yeats and others, 1996; Tolan and Beeson, 1999).

The Troutdale Formation in the Woodland quadrangle contains sparse clasts of pyroxene andesite that probably were eroded from middle to late Miocene volcaniclastic units in the Columbia River Gorge, but lacks clasts of distinctive olivine-phyric, high-alumina basaltic rocks that erupted within the gorge mainly after 3.5 Ma (Conrey and others, 1996a, b). The clast composition indicates the conglomerate in the map area is equivalent to the informal lower member of the Troutdale Formation of Tolan and Beeson (1984) in the Columbia River Gorge (fig. 4), for which an age of middle to late Miocene was inferred. Tolan and Beeson (1984) based this age range on correlations with plant-bearing outcrops west of the gorge. However, complex facies changes in the intervening area between the Columbia River Gorge and the Woodland area (Bet and Rosner, 1993; Swanson and others, 1993) render such lithologic correlations problematic. Given this uncertainty and the poor age resolution of plant fossils, an age as young as early Pliocene for the Troutdale Formation in the map area is permissible.

Therefore, based on the meager evidence, the age of the Sandy River Mudstone in the Portland Basin is considered to range from late early Miocene to early Pliocene. The eroded top of the unit in the Woodland quadrangle suggests that only the older, Miocene part of the formation is preserved here. The age of the Troutdale Formation in the map area is considered to be late Miocene and (or) early Pliocene.

### UNNAMED CONGLOMERATE

Conglomeratic beds that are believed to be younger than the Troutdale Formation crop out at lower elevations near the southern boundary of the Woodland quadrangle (QTc). Outcrop and subsurface data demonstrate that these beds are at the northern margin of a sheetlike body of conglomerate 20 to 40 m thick that can be traced throughout much of Clark County (Mundorff, 1964; Swanson and others, 1993). In the northern Portland Basin, these beds lap against the Sandy River Mudstone with slight discordance, demarking a significant erosional unconformity. The conglomerate is less deeply weathered than the older Troutdale Formation, but is texturally similar to it, being characterized by crude stratification, coarse grain size, moderate to good sorting, openwork and sand matrix, and well-developed clast imbrication, and reflects deposition in a similar fluvial setting. The conglomerate contains a higher proportion of Paleogene volcanic rocks eroded from the adjacent Cascade Range, however. Furthermore, it is distinguished by the presence of sparse clasts of high-alumina olivine-bearing basalt, which erupted from the Cascade Range only during past 3.5 m.y. (Tolan and Beeson, 1984; Conrey and others, 1996a, b) and thus constrains the maximum depositional age of the conglomerate to late Pliocene. Correlative conglomerate to the southeast was suggested by Howard (2002) to include probable outwash; if so, deposition may have continued into the Pleistocene.

## QUATERNARY DEPOSITS

The Lewis River Basin occupies about 3000 km$^2$ of the southern Washington Cascade Range. The river heads on Mount Adams, about 95 km east-northeast of the map area, and drains the southern flank of Mount St. Helens. As noted by Major and Scott (1988), Quaternary sedimentation in the lower Lewis River valley has been influenced by several processes, chief of which are: (1) variations in base level owing to sea level fluctuation, (2) episodes of mountain glaciation, (3) inundation by cataclysmic jökulhlaups (glacier outburst floods), and (4) eruptive activity at the stratovolcanoes.

## GLACIAL AND RELATED DEPOSITS

Several times during the Pleistocene epoch, icecaps covered the Washington Cascade Range and spawned glaciers that moved down all of the major river valleys. From examinations of glacial deposits near Mount Rainier, Crandell and Miller (1974) inferred four major glacial episodes, each of which apparently consisted of several lesser advances and retreats (Dethier, 1988). The most widespread glacial deposits in the Cascade Range are those attributed to the penultimate glaciation, the Hayden Creek Drift of Crandell and Miller (1974). Deeply weathered older deposits, the Wingate Hill Drift and the Logan Hill Formation, are locally preserved in the western Cascade foothills in areas beyond the reach of Hayden Creek glaciers. The last major glaciation in western Washington was the Fraser glaciation; deposits of this age in the Cascade Range, named the Evans Creek Drift, are much less extensive than those of the Hayden Creek age (Crandell and Miller, 1974; Crandell, 1987). Mundorff (1964) mapped widely distributed till and glaciofluvial sediments throughout the lower Lewis River valley; he later formally named these deposits the Amboy Drift and correlated them with the Hayden Creek Drift of the Mount Rainier region on the basis of similar weathering characteristics (Mundorff, 1984). However, Crandell (1987) noted that some of the till in Mundorff's (1984) Amboy Drift near Battle Ground was more deeply weathered than typical Hayden Creek Drift, and suggested that the Amboy Drift as mapped by Mundorff (1964, 1984) includes some much older drift (Crandell, 1987; see also Howard, 2002). Evarts (2004) mapped these two drifts in the Ariel quadrangle. He restricted the name Amboy Drift to deposits considered correlative with the Hayden Creek Drift of Crandell and Miller (1974), and informally named the older, more deeply weathered deposits the drift of Mason Creek. In the Woodland quadrangle, unconsolidated glaciofluvial deposits that were mapped as Amboy Drift by Mundorff also exhibit significant variations in weathering, as well as minor but important differences in clast composition, and appear to represent at least two major glacial advances.

### Glacial deposits older than the Amboy Drift

Stratified sand and gravel (Qmo) form moderately to highly dissected terraces with surface elevations near 400 ft (120 m) along the north flank of Goose Hill and 2 to 3 km east of Hayes. Similar deposits crop out at several locations north of the Lewis River and are common to the east in the Ariel quadrangle. The terrace deposits are weathered to depths of at least 4 m, deeply oxidized, and commonly limonite cemented; weathering rinds on aphanitic andesite clasts are 2 to 15 mm thick, averaging about 6 mm. These deposits thus appear to be much older than the Amboy Drift. The gravels consist largely of well-rounded cobbles and pebbles of volcanic rocks similar to those exposed in the adjacent the Cascade Range, indicating a Lewis River source. No clasts attributable to the Mount St. Helens volcanic center occur in these sediments, but they locally contain a few cobbles of olivine-phyric basalt or basaltic andesite that were probably eroded from small volcanic centers mapped in the Lewis River valley to the northeast of the Woodland quadrangle by Evarts and Ashley (1990a, 1991). Whole-rock $^{40}Ar/^{39}Ar$ ages of these mafic centers range from 622 to 779 ka (R.J. Fleck, written commun., 2003, 2004), which provides a maximum age for the gravel. The deeply weathered terrace sediments are interpreted as glaciofluvial outwash related to one or more episodes of early or middle Pleistocene glaciation. Weathering characteristics resemble those of the Wingate Hill Drift of Crandell and Miller (1974), the age of which is estimated to be 300 to 600 ka by Colman and Pierce (1981) and Dethier (1988). Crandell (1987), however, believed that similarly weathered till at a locality about 7 km southeast of Highland might be somewhat older than the Wingate Hill Drift near Mount Rainier.

Gravel (Qoo) that may be the remains of a thick glaciofluvial deposit older than the drift of Mason Creek (Qmo) overlies the Troutdale Formation about 4 km north of Woodland. The gravel consists entirely of Cascadian volcanic rocks and lacks quartzite or Columbia River Basalt Group clasts, so was deposited by the ancestral Lewis River rather than by the Columbia River. Although similar to the drift of Mason Creek in clast lithology and weathering characteristics, the gravel is found at a much higher elevation, up to nearly 600 ft (180 m) in the adjacent Deer Island quadrangle (Evarts, 2002). It is, therefore, tentatively interpreted as the remnant of an older alluvial fill possibly related to an early Pleistocene glacial advance.

Fluvial sediments (Qtd) that may be correlative, in part, with the pre-Amboy Drift outwash of the Lewis River valley form several small terrace remnants banked against the bedrock slope at the eastern edge of the Columbia River floodplain southeast of Woodland. The terraces consist largely of gravel, sand, and silt mantled by micaceous silt deposited by the Missoula floods (Qfs). Clasts in the sediments are predominately Tertiary volcanic rocks of Cascade Range derivation, with little or no Columbia River Basalt Group or quartzite; this suggests they were deposited by the Lewis River rather than by the Columbia. Mundorff (1964) mapped these deposits as Troutdale Formation but their composition, geomorphology, and relatively low elevation indicate they are younger, as inferred by Swanson and others (1993).

A 6-m-thick lens of laminated, white, fresh volcanic ash crops out in a slump-scarp exposure of terrace deposits (Qtd) on the bank of the Lewis River directly east of the Interstate Highway 5 bridge. The thickness and lensoidal nature of the ash deposit indicates it is of fluvial rather than airfall origin. The chemistry of glass shards in the ash corresponds to that of the Bend Pumice and Loleta ash bed (A.M. Sarna-Wojcicki, written commun., 2000), which were produced by a large eruption in the central Oregon Cascade Range between 350 and 450 ka (Hill and Taylor, 1989; Sarna-Wojcicki and others, 1989; Lanphere and others, 1999). Because prevailing winds during this eruption carried tephra to the south and west of the eruptive center (A.M. Sarna-Wojcicki, written commun., 2000), the ash deposit probably consists of riverborne ash transported from the eruption site into the Columbia drainage by the Deschutes or Willamette Rivers, not of material reworked from a local airfall blanket. The exceptional purity of the ash suggests that the lower Columbia system was temporarily overwhelmed by a massive influx of freshly erupted pyroclastic debris. Large amounts of tephra were evidently flushed downstream shortly after the paroxysmal eruption, and some of it was deposited in overbank settings at the margin of the Columbia River floodplain. The inferred age of the ash is within the range estimated for the Wingate Hill Drift (Colman and Pierce, 1981; Dethier, 1988), suggesting that the terrace deposits may be partly correlative with the drift of Mason Creek outwash (Qmo) mapped in the Lewis River valley. The surfaces of the terrace remnants are more than 60 m lower than that of the terrace north of Goose Hill, but they may be erosional surfaces that reflect postglacial downcutting by the Columbia River of a thick outwash apron formed at the mouth of the Lewis River during Wingate Hill time.

### Amboy Drift

Outwash sands and gravels that possess weathering characteristics like those described for the Amboy Drift (Qao) and correlative Hayden Creek Drift (Crandell and Miller, 1974; Mundorff, 1984; Crandell, 1987) are relatively sparse in the Woodland quadrangle compared to areas to the east. They form isolated terrace remnants on both sides of the Lewis River, inset against older and more weathered deposits. The surface elevations of these terraces are near 200 ft (60 m). The gravels contain well-rounded pebbles and cobbles, some with grooved or striated surfaces, of diverse volcanic rocks similar to Tertiary rocks in the Lewis River Basin; quartzite and Columbia River Basalt Group clasts are absent. Some outcrops contain sparse cobbles of olivine-phyric basalt and basaltic andesite similar to lavas erupted from early and middle Pleistocene volcanic vents in the Lewis drainage northeast of the quadrangle (Evarts and Ashley, 1990a, 1991). Clasts of distinctive, coarsely porphyritic quartz-, biotite-, and cummingtonite-bearing dacite are a minor but persistent component in the gravels. The only known source for this rock type in the region is the volcanic center of Mount St. Helens (Crandell, 1987), and the presence of the dacite in the Amboy Drift implies that eruptive activity began during or before Hayden Creek time.

The numerical ages of Hayden Creek Drift and its local equivalent, the Amboy Drift, are poorly known. Estimates range from 60 ka to greater than 300 ka (Crandell and Miller, 1974; Colman and Pierce, 1981; Crandell, 1987; Dethier, 1988; Grigg and Whitlock, 2002). Stratigraphic relations in the Cowlitz River valley about 65 km north of the Woodland quadrangle (Dethier, 1988) and in the Lewis River valley east of the map area (Evarts and others, 2003; Evarts, 2004; R.C. Evarts, unpub. mapping) indicate that glacial deposits with the weathering characteristics of the Hayden Creek Drift probably represent two or three separate advances during this time.

## ALLUVIUM DERIVED FROM MOUNT ST. HELENS VOLCANIC CENTER

The Lewis River drains the southern slope of Mount St. Helens, which is approximately 30 km upstream from the Woodland quadrangle. Eruptive activity at the volcanic center has been the dominant influence on sedimentation in the lower Lewis valley in postglacial time. Pyroclastic flows and lahars generated by eruptions of the volcano have moved down the valley many times during its history (Crandell, 1987; Major and Scott, 1988). No pyroclastic flows or lahars are known to have reached as far downvalley as the Woodland quadrangle, but sand and gravel composed of fluvially reworked Mount St. Helens debris forms several terraces along the river upstream from the town of Woodland. These terrace deposits probably record aggradational events triggered by the influx of large volumes of volcaniclastic debris introduced upvalley by eruptive activity at the volcano (Major and Scott, 1988).

Crandell (1987) showed that eruptive activity at Mount St. Helens was episodic and can be divided into several eruptive stages and periods (fig. 5), the products of which commonly can be distinguished on the basis of lithology

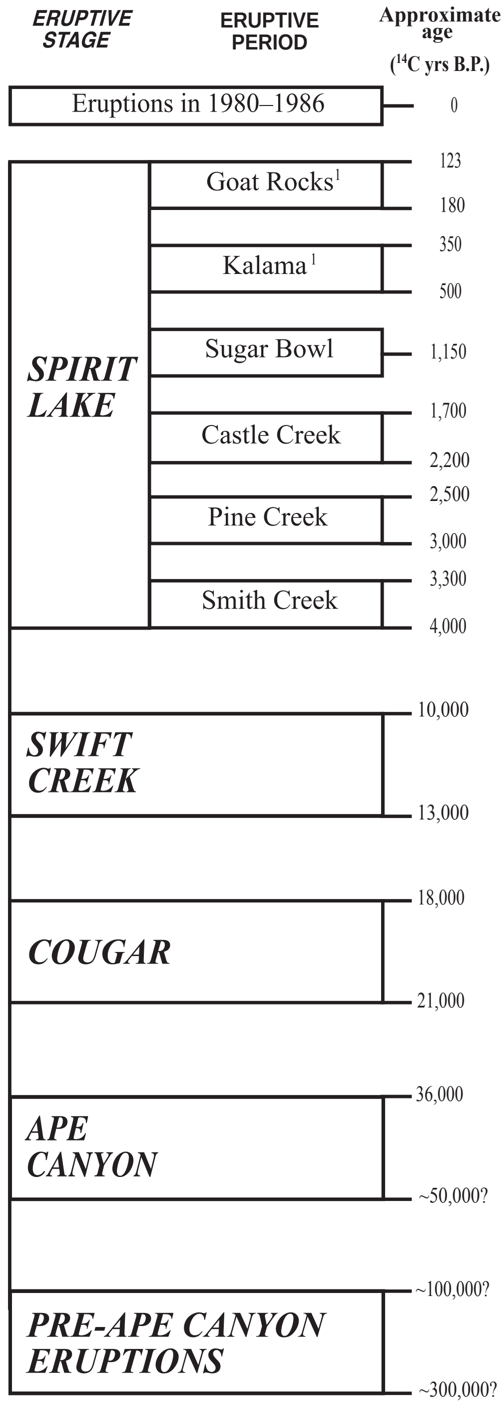


[1]Ages for Goat Rocks and Kalama eruptive periods are in calendar years before A.D. 1950 based on tree-ring and radiocarbon dates and historical records

**Figure 5.** Eruptive stages and eruptive periods of Mount St. Helens volcano, modified from Crandell (1987).

and phenocryst assemblages. Because of poor exposure, it was not possible to assign the fragmentary alluvial deposits in the Woodland quadrangle to specific subdivisions of Crandell's Mount St. Helens eruptive history. Instead, the Mount St. Helens-derived alluvium unit (Qsh) shown on this map consists of those sediments whose lithology and stratigraphic position indicate they predate the latest Pleistocene cataclysmic floods (Qfs) of about 17,000 and 13,000 $^{14}C$ yrs B.P. (Waitt, 1985, 1994; Clague and others, 2003); younger deposits of similar character are included with Holocene alluvium (Qa; see below).

Pre-flood Mount St. Helens alluvial deposits form terrace remnants on both sides of the Lewis River valley; surface elevations of the pre-flood terraces vary from 60 to 230 ft (18 to 70 m). Although some beds contain significant amounts of debris eroded from Tertiary volcanic rocks and the Troutdale Formation, their clast population is typically dominated by Mount St. Helens dacites. Mount St. Helens dacites are readily distinguished from Paleogene silicic rocks by their light-gray to pink colors, densely and coarsely porphyritic textures, and the presence of amphibole phenocrysts. The most common clast type observed in the gravel beds of terrace sections is quartz- and biotite-phyric dacite, a rock type produced only by the earliest eruptions at the Mount St. Helens, before about 36,000 $^{14}C$ yrs B.P. (fig. 5). This suggests that much of the alluvium of the terraces is correlative with the Ape Canyon-age and older fill that is locally preserved upvalley (Major and Scott, 1988; Evarts, 2004; R.C. Evarts and M.A. Clynne, unpub. mapping). Gravel in the terrace directly north of Woodland contains clasts of hypersthene-hornblende dacite in addition to biotite-bearing dacite; the former are typical products of the Cougar eruptive stage, roughly 21,000 to 18,000 $^{14}C$ yrs B.P. (fig. 5). This terrace may therefore be a downvalley equivalent of thick Cougar-age deposits that fill a Lewis River paleochannel between Lake Merwin and Yale Lake (Major and Scott, 1988; R.C. Evarts and M.A. Clynne, unpub. mapping).

## CATACLYSMIC FLOOD DEPOSITS

During the last glacial maximum in late Pleistocene time, an ice dam impounded Glacial Lake Missoula in western Montana. The dam failed repeatedly, releasing enormous floods or jökulhlaups, commonly referred to as the Missoula floods, that coursed down the Columbia River and into the Portland Basin (Bretz, 1925, 1959; Bretz and others, 1956; Trimble, 1963; Allison, 1978; Baker and Bunker, 1985; Waitt, 1985, 1994, 1996; O'Connor and Baker, 1992; Benito and O'Connor, 2003). The sediment-laden floodwaters were hydraulically constricted by the relatively narrow reach of the Columbia River valley between Kelso and Kalama, just north of the Woodland quadrangle. The constriction caused temporary ponding in the Portland Basin and tributary valleys, such as the Lewis River, to levels as high as 400 ft (120 m). Radiocarbon ages, paleomagnetic measurements, and tephrochronologic data indicate that the last-glacial episode of floods occurred chiefly between about 17,000 and 13,000 $^{14}C$ yrs B.P. (Waitt, 1985;1994; Atwater, 1986; Clague and others, 2003). Similar episodes of cataclysmic flooding probably occurred earlier in the Quaternary (McDonald and Busacca, 1988; Zuffa and others, 2000; Bjornstad and others, 2001).

During each flood, the suspended load of fine sand and silt settled out of the temporarily ponded floodwaters. In the northern Portland Basin, multiple floods (Waitt, 1994, 1996) collectively built up deposits of laminated micaceous sediments as thick as 30 m. Silty slack-water flood deposits (Qfs) underlie terrace surfaces along both sides of the Lewis River valley upstream from Woodland, and unmapped thin flood deposits locally mantle the topography to elevations as high as 400 ft (120 m). A broken boulder of very coarse-grained granitic rock, interpreted as an ice-rafted erratic, was found on the surface at an elevation of 340 ft (105 m) near Cardai Hill. The laminated character of the flood deposits is obvious only in fresh slump-scarp outcrops because oxidation colors exposures light brown and obscures bedding. They are dominated by grains of quartz and feldspars and contain conspicuous muscovite, which confirms their Columbia River provenance.

## HOLOCENE ALLUVIAL DEPOSITS

A thick fill of unconsolidated alluvium (Qa) underlies the Lewis River valley floor near Woodland. East of the map area, the Lewis River flows through a narrow channel confined between steep walls of Paleogene bedrock. Near the eastern edge of the quadrangle, the river emerges from this channel and meanders across a 1-km-wide floodplain that is underlain chiefly by silt, sand, and gravel. At Woodland, these deposits interfinger with finer grained sediment of the modern Columbia River floodplain (Gates, 1994). In contrast to the Columbia River deposits, which contain a substantial nonvolcanic component (Whetten and others, 1969; Gates, 1994), recent Lewis River sediments are overwhelmingly volcaniclastic, consisting largely of Tertiary bedrock clasts supplemented by significant quantities of debris derived from Mount St. Helens. Flanking the areas of active alluvium along the river are several low terraces, some of which probably formed in response to eruptive events at Mount St. Helens during the past 1000 years (Major and Scott, 1988). The most prominent terrace, about 6 to 8 m above the modern river, was named the Woodland terrace by Major and Scott (1988), who inferred that it records aggradation during the Kalama eruptive period of Mount St. Helens (fig. 5). Water-well logs indicate there is at least 75 m of unconsolidated sediments beneath Clover Valley and more than 80 m beneath Woodland. Most of these sediments were probably deposited since the latest Pleistocene lowstand in sea level (Warne and Stanley, 1995; Clark and Mix, 2002) but pre-Holocene sediment may be present at depth.

### LANDSLIDE AND TALUS DEPOSITS

Landslides (Qls) are distributed throughout the steeper terrain of the Woodland quadrangle. Most result from failure of clay-rich Paleogene volcaniclastic sedimentary rocks and tuffs (Tvs, Tt, and unmapped sedimentary interbeds within flow-dominated units Tba and Ta) or of younger, poorly lithified deposits. The Sandy River Mudstone (Tsr), where overlain by the Grande Ronde Basalt, is particularly susceptible to collapse, and several slides have developed in this unit southeast of Woodland. Fiksdal (1975) considered these slides stable, but recent continued movement is apparent in several of them, including one opposite the Lewis River from the Woodland Airport (Harp and others, 1997). This slide crossed the Old Pacific Highway in 1996 and blocked it for several months. Slumping is also common along the steep edges of terraces that are made up of unconsolidated cataclysmic flood (Qfs), Mount St. Helens (Qsh), and outwash deposits. In 1997, a section of the terrace margin along the Lewis River east of Hayes collapsed, requiring the relocation of County Route 16. Piecemeal breakup of cliff-forming units produced the talus deposits on the east flank of Devils Peak. Only the larger landslides are shown on this map; most areas underlain by Quaternary units and the Troutdale Formation also contain small slumps and debris-flow deposits that are too small to portray at 1:24,000 scale.

## STRUCTURAL FEATURES

Paleogene strata in the Woodland quadrangle generally strike east-northeast and dip 15° to 30° south-southeast and form the western limb of a broad, south-plunging syncline whose axis is located to the east in the adjacent Ariel quadrangle (Evarts, 2004). The syncline belongs to a regional system of large north- to northwest-trending folds in the southern Washington Cascade Range that probably developed during late early Miocene time (Evarts and Swanson, 1994). Immediately west of the Woodland quadrangle, the strike of the Paleogene strata bends sharply northwest (Evarts, 2002), defining a north-trending, south-plunging anticlinal axis that is located near Green Mountain. Evarts (2002) and Evarts and others (2002) suggest that this structure is a large drag fold created by clockwise rotation (and westward tilting?) within a complex zone of dextral shear located near the Columbia River northwest of Woodland.

The swarm of subvertical to steeply north-dipping dikes that intrude Paleogene rocks north of the Lewis River is approximately 3 km wide north of Woodland and widens to the east. It continues, with individual dikes maintaining the same N. 75° E. preferential orientation, eastward at least 6 km into the adjacent Ariel quadrangle (R.C. Evarts, unpub. mapping). The swarm is spatially associated with a broad area of dioritic plutonic rocks centered in the Ariel quadrangle, but the uniform orientation of the dikes over such a large area probably reflects regional tectonic forces rather than localized stresses related to emplacement and growth of a magmatic focus. Most dikes dip northward at about 70° (see cross sections); restoring the south-southeast dipping host strata to a horizontal orientation rotates the dikes to nearly vertical. Assuming the dikes were originally vertical conduits, folding thus postdates dike intrusion.

High-angle normal and strike-slip faults of variable orientation break the Paleogene bedrock sequence into a number of blocks. Owing to the limited outcrops in this quadrangle, direct evidence for the existence of faults is sparse. Some faults are projected from structures observed in roadcuts or natural exposures. Others are inferred from apparent discontinuities in distinctive units at the surface or in well records, from topographic lineaments, from abrupt changes in bedding trends, or from aeromagnetic anomalies. None appear to be major regional structures. Vertical displacements, inferred from offset stratigraphic contacts, are typically less than 200 ft; horizontal displacements are difficult to quantify but are probably of similar magnitude. The fault pattern of the map area is characteristic of southwestern Washington (Wells, 1981; Wells and Coe, 1985; Evarts and Ashley, 1991, 1992;

Evarts and Swanson, 1994; Evarts, 2002, 2004; R.C. Evarts, unpub. mapping) and these structures are believed to accommodate the paleomagnetically recorded rotations of crustal blocks in response to oblique convergence along the Cascadia Subduction Zone (Wells and Coe, 1985; Wells, 1989, 1990; Beck and Burr, 1979; Bates and others, 1981; Hagstrum and others, 1999).

Oblique subduction has been characteristic of Cascadia throughout Cenozoic time (Engebretson and others, 1985; Verplanck and Duncan, 1987; Wells, 1990). Consequently, movement on the block-bounding faults presumably is of a similar age range. In the map area, however, the ages of most faults are poorly constrained because they offset no rocks younger than late Eocene. Some faults are occupied by undeformed dikes or by zeolite veins and thus have not been active since the last magmatic or hydrothermal activity in this area, probably during the Oligocene. Other fault-controlled dikes, however, exhibit post-intrusion movement. Southeast of Woodland, a northwest-striking normal fault offsets the early middle Miocene Grande Ronde Basalt and, possibly, the late Miocene Sandy River Mudstone. The base of the unassigned reversely magnetized flow is about 200 ft lower southwest of the fault, but the exact amount of offset is uncertain because the basal contact is an erosional unconformity and its original configuration is unknown.

Scant evidence for Quaternary deformation was found in the Woodland quadrangle. Gentle folding of the conglomerate unit (QTc) in the Portland Basin was inferred by Swanson and others (1993) and Bet and Rosner (1993) based on variations in the elevations of subsurface contacts. Grande Ronde Basalt flows exposed in the west-facing escarpment that bounds the Columbia River floodplain southeast of Woodland match flows at similar elevations in northwestern Oregon, indicating that the flows once extended across the Columbia River valley. The intervening basalt was probably eroded away, but alternatively, may have been dropped beneath the modern floodplain by post-Miocene warping or extensional faulting. Based on geologic, paleomagnetic and areomagnetic data, Evarts (2002) and Evarts and others (2003) suggest that the northern Portland Basin lies within a complex zone of dextral shear. Several north- and northwest-striking faults, interpreted from areomagnetic anomalies, are inferred to underlie Holocene sediments west of Woodland, and the linear escarpment southeast of Woodland may reflect control by one of these structures. However, any scarps produced by recent faulting are probably short-lived in the active Holocene floodplain of the Columbia River.

## GEOLOGIC EVOLUTION

Previous regional studies have shown that the Portland Basin and its bounding structures have a long and complex tectonic history (Beeson and others, 1989; Blakely and others, 1995; Yeats and others, 1996). Beeson and Tolan (1990) suggest that development of the structure that evolved into the present basin began in late early Miocene time, shortly before flows of the Grande Ronde Basalt entered western Oregon and Washington. Considerable evidence also exists for older regional deformation (Snavely and Wells, 1996; Niem and others, 1992, 1994). Data from the Woodland quadrangle provide additional insights into the nature and timing of basin evolution.

The general character of late Eocene bedrock in the Woodland quadrangle, with its thick sections of lava flows, plug-dome complexes, coarse-grained breccias, pumiceous pyroclastic rocks, and scattered intrusions, typifies central vent and proximal volcanic environments within continental volcanic arcs (Williams and McBirney, 1979; Vessel and Davies, 1981; Cas and Wright, 1987; Orton, 1996). Regional relations indicate that this area occupied the west margin of the active Cascade volcanic arc during Paleogene time. Age determinations in adjacent quadrangles (Evarts, 2002; R.J. Fleck, written commun., 2000) show that the extrusive rocks in the map area were deposited mainly between 35 and 37 Ma, early in arc history (Duncan and Kulm, 1989; Evarts and Swanson, 1994).

The oldest rocks exposed in the quadrangle are subaerially emplaced basaltic andesite flows in the northwestern quadrant that probably formed the flank of a large mafic shield volcano. Small areas of brick-red scoria exposed in Burris Creek and the Little Kalama River may be remnants of cinder cones that grew on the flanks of this volcano. Thick flow-dominated sections at higher stratigraphic levels, such as the hypersthene basaltic andesite (Thba) and the andesitic pile at Goose Hill, resemble lava accumulations that commonly form the lower flanks of stratovolcanoes or fill near-vent canyons. The thick pile of pyroclastic rocks in the Butte Hill area may have accumulated within a valley eroded into the older mafic shield or may have filled a crater or small caldera, perhaps associated with the dacitic center near the mouth of Robinson Creek. In contrast, the sequences of interbedded pyroclastic deposits and finer grained, stratified volcaniclastic sedimentary rocks in the northeastern part of the map area record deposition in medial to distal settings beyond the flanks of active volcanic edifices (Williams and McBirney, 1979; Vessel and Davies, 1981).

Although they have not been dated, the fine-grained dikes, sills, and plugs in the Woodland quadrangle are probably only slightly younger than their lithologically similar extrusive host rocks, and some may occupy vents that fed now-eroded volcanoes. Coarser grained dioritic bodies in the eastern part of the quadrangle are satellitic to a major magmatic center to the east (Evarts, 2004). The age of these rocks is also unknown, but they are interpreted to represent late-stage magmatism associated with a caldera complex in the adjacent Ariel quadrangle. Some dioritic intrusions may have fed late Eocene or Oligocene volcanoes that have since been completely eroded away. If so, removal of the superjacent rocks most likely occurred in late early Miocene time during an episode of uplift and regional folding in southern Washington (Evarts and Swanson, 1994). This episode produced the large north- to northwest-trending folds that characterize the southwestern part of the Cascade Range in southern Washington (Evarts and Swanson, 1994). The most intense phase of this event was largely over by about 16 Ma because south-dipping Paleogene rocks near Woodland are unconformably overlain by essentially flat-lying semiconsolidated sedimentary strata and Grande Ronde Basalt flows of that age.

Development of the Portland Basin apparently began at about the same time as the early Miocene regional folding event (Beeson and others, 1989; Beeson and Tolan, 1990). At this time, western Washington and Oregon constituted a terrain of modest relief (Wilkinson and others, 1946; Beeson and others, 1989), and the course of the ancestral Columbia River through the region was determined by a combination of subtle structural controls and differential erosion of various Paleogene volcanic and sedimentary rocks. Fine-grained nonmarine sediments of the Sandy River Mudstone, which record deposition in low-energy fluvial and lacustrine environments, began to accumulate in the incipient Portland Basin and similar settings to the south and west (Van Atta and Kelty, 1985; Beeson and others, 1989; Tolan and Beeson, 1999). The absence of coarse-grained volcaniclastic debris signifies that the middle Miocene Cascade arc was topographically subdued and volcanically quiescent compared to earlier times. The earliest flood-basalt flows to enter western Oregon and Washington region commonly exhibit invasive relations with these sediments. This demonstrates that the sediments were unconsolidated and probably water saturated at the time, implying that little time elapsed between sedimentation and arrival of the lava flows.

Beginning about 16.5 Ma, flood-basalt flows of the Grande Ronde Basalt entered the Portland Basin in rapid succession by way of a 60-km-wide lowland transecting the Cascade Range; the basin was large enough by this time to affect the flow paths of the basalt flows through western Oregon (Tolan and others, 1989; Beeson and others, 1989; Beeson and Tolan, 1990). Early Grande Ronde flows filled the ancestral Columbia River valley, leaving a nearly flat surface that permitted later flows to spread widely throughout the region (Beeson and others, 1989). The presence of flood-basalt outcrops on both sides of the Columbia River valley near Woodland (Evarts, 2002) indicates that the ancestral valley here was once filled with basalt, most of which has been eroded away by the Columbia River. At least two flows (Tggc(?) and Tgww) interacted with tributary streams flowing westward out of the ancestral Cascade Range to produce local accumulations of pillow lava and basaltic hyaloclastite (Tbh). The younger Winter Water and Sentinel Bluffs flows (Tgww and Tgsb) are inset against the older reversely magnetized basalt, indicating that a period of fluvial incision separated their emplacement. The basalt remnants are banked against a steep slope cut in Paleogene rocks; the Columbia River valley wall of late early Miocene time was thus located in essentially the same location as the modern valley margin. The steep linear valley margin in this area may reflect offset on an early basin-bounding fault zone. Post-Grande Ronde Basalt eruptions were relatively infrequent, allowing the Columbia River to erode canyons into the older basalt flows (Beeson and others, 1989). Later Columbia River Basalt Group flows were largely confined to these new canyons, which were located west of the Woodland quadrangle (Tolan and others, 1989; Evarts, 2002).

Sediments in the Portland Basin that immediately postdate the Miocene flood basalts are similar in character to the fine-grained deposits that underlie the lava flows near Woodland. This indicates that, aside from temporary and local perturbations imposed by emplacement of the flows, the regional sedimentary regime remained essentially unchanged into late Miocene time. The mineralogy of Sandy River Mudstone beds indicates a primary source area in pre-Tertiary plutonic and metamorphic terranes east of the Cascade arc, with minor contributions from volcanic activity in the arc. Several workers have suggested that the fluvial and lacustrine deposits of the ancestral Columbia River in the Portland Basin accumulated near sea level (Lowry and Baldwin, 1952; Mundorff, 1964; Beeson and Tolan, 1990), although marine fossils have not been reported. Mundorff (1964) states that a few water wells to the southeast of Woodland encountered salty water in the sandstone and siltstone facies of the Troutdale Formation, consistent with a shallow-marine or brackish water environment. To the southeast, near the western end of the Columbia River Gorge, these sandy and silty beds grade laterally into conglomeratic fluvial deposits (Tolan and Beeson, 1984; Swanson and others, 1993; Bet and Rosner, 1993). If all these sediments were deposited near sea level, the floor of the Portland Basin must have gradually subsided as they accumulated; the basin floor now lies as much as 1800 ft (550 m) below sea level (Swanson and others, 1993).

Subsurface data east of Goose Hill reveal a paleovalley incised into Paleogene bedrock and filled with Miocene sediments. According to Swanson and others (1993), the floor of the paleovalley lies near present sea level. The origin of this feature is unknown. It may have been carved by the ancestral Columbia River after its valley was filled with the 12-Ma Pomona flow (Tolan and Beeson, 1984), forcing the river to the eastern margin of the basalt-filled valley. Alternatively, it may record the late Miocene course of an ancestral Lewis River.

In the southern part of the Woodland quadrangle, the fine-grained basin-fill strata of the Sandy River Mudstone are disconformably overlain by conglomeratic beds of the Troutdale Formation (Trimble, 1963; Mundorff, 1964; Swanson and others, 1993). Clasts eroded from flows of the Miocene Columbia River Basalt Group constitute the predominant component of these gravelly beds, but they also contain clasts of granitic, metamorphic, and quartzite rocks derived from pre-Tertiary terranes east of the Cascade Range as well as sparse clasts of pyroxene andesite that were probably eroded from Miocene volcaniclastic units in the Columbia River Gorge. The superposition of the Troutdale Formation on the Sandy River Mudstone evidently records the northward progradation of a gravelly braid-plain across the Portland Basin during late Miocene or early Pliocene time. This pronounced change in the Columbia River sedimentary regime may record regional uplift to the east and initial incision of the Columbia River Gorge. The dissected, gently sloping surface of the Troutdale Formation apparently was tilted southwestward during Pliocene uplift of the Cascade Range. As a result, the Columbia River incised its floodplain and eroded the late Miocene gravel from much of the northern Portland Basin, leaving remnants preserved only on its uplifted flanks.

The unnamed conglomerate unit (QTc) represents a younger episode of gravel deposition in the Portland Basin. The sedimentology of this deposit implies deposition by torrential floods in a braided stream environment (Miall, 1977, 1996; Rust, 1978; Ramos and Sopeña, 1983). Clasts eroded from flows of the Columbia River Basalt Group predominate, indicating deposition chiefly by the ancestral Columbia River. Tertiary volcanic rocks eroded from the Cascade Range are abundant in the conglomerate near the eastern margin of the Portland Basin, however. Hence, the Cascade Range had been elevated and was also contributing coarse sediment by this time. The widespread presence of high-alumina olivine-basalt cobbles indicates the conglomerate was probably deposited during late Pliocene to early Pleistocene time (Tolan and Beeson, 1984).

A complex assemblage of Quaternary deposits in the lower Lewis River valley records alternating periods of alluviation and downcutting in response to variations in sediment load and fluctuations in sea level (Mundorff, 1984; Major and Scott, 1988). The Troutdale Formation at one time likely extended northward and lapped onto Paleogene bedrock north of the modern Lewis River. Continuing uplift of the Cascade Range rejuvenated the ancestral Lewis River, which, by early Pleistocene time, had removed much of the Troutdale Formation sediments and cut a deep valley into the subjacent bedrock. Subsequently, mountain glaciers advanced out of the Cascade Range and down the Lewis River valley several times. Evidence for early and middle Pleistocene glacial advances in the Lewis drainage basin was largely erased by the glaciation(s) that deposited the Amboy Drift, the local correlative of the Hayden Creek of Crandell and Miller (1974). The Amboy-age glacier terminated just east of the Woodland quadrangle (Mundorff, 1964; Evarts, 2004). Deeply weathered probable outwash deposits (Qmo and Qoo) in the lower Lewis River valley record one or more major pre-Amboy glaciations. These alluvial deposits predate the inception of Mount St. Helens but contain clasts similar to early Pleistocene olivine-phyric basalts erupted from vents in the Cascade Range to the east. Some of these deposits may correlate with the Wingate Hill Drift of Crandell and Miller (1974), based on their similar weathering characteristics, or they may be older. Fragments of an Amboy-age, proglacial outwash train are locally preserved as lower terrace remnants. These deposits (Qao) locally contain clasts of distinctive quartz-, biotite-, and cummingtonite-bearing porphyritic dacite produced by the earliest eruptions at ancestral Mount St. Helens. The most recent glaciation in the Cascade Range, which culminated about 17 ka (Barnosky, 1984), was considerably less extensive than the Hayden Creek (Amboy) advance, and left no identifiable deposits in the lower Lewis River valley.

Mount St. Helens erupted frequently during and after the Hayden Creek glaciation (Crandell, 1987; Evarts and others, 2003). Most of these events have been explosive, and some have dumped huge quantities of pyroclastic debris into the Lewis River system. Evidence for periods of eruption-induced aggradation and subsequent incision by the river is abundant east of the Woodland quadrangle (Major and Scott, 1988; Evarts, 2004; R.C. Evarts and M.A. Clynne, unpub. mapping). Deposits of Mount St. Helens origin that are exposed in the map area consist of fluvially transported sand and gravel reworked from primary eruptive deposits upstream. They form low terrace remnants within the Lewis River valley, most of which are topped by thick cataclysmic flood deposits. Water-well data indicates that Mount St. Helens-derived sediment also constitutes a substantial proportion of the alluvial fill beneath the modern flood plain; much of this debris was probably deposited when the river's base level was lower during the latest Pleistocene sea-level lowstand.

Near the end of the Pleistocene, about 17,000 to 13,000 $^{14}C$ yrs B.P., the lower Lewis River valley, like the rest of the Portland Basin region, experienced cataclysmic flooding initiated by failure of an ice dam impounding Lake Missoula in Montana (Bretz, 1959; Waitt, 1985). These jökulhlaups, or outburst floods, left behind silty slack-water deposits that mantle land surfaces as high as 400 ft (120 m) in the map area. Repeated floods during a few-thousand-year span built up deposits of laminated silt and fine sand as much as 30 m thick that are preserved throughout the lower Lewis River valley on terrace surfaces well above the modern floodplain. Sea level at the end of the Pleistocene was about 50 to 60 m lower than at present (Warne and Stanley, 1995; Clark and Mix, 2002), and the Columbia and Lewis Rivers had correspondingly lower base levels. During the subsequent rapid sea-level rise, aggradation in the lower Columbia valley generally kept pace with the rise in sea level (Gates, 1994); presumably sedimentation in the Lewis valley did so as well.

## GEOLOGIC RESOURCES

Geologic resources available in the Woodland quadrangle are limited to nonmetallic industrial materials, chiefly aggregate for construction purposes. Although hydrothermal alteration similar to that observed in the northern Woodland quadrangle is commonly associated with metallic mineral deposits in the Cascade Range, no significant mineral occurrences were found. Paleogene volcanic bedrock has locally been quarried for crushed aggregate, used primarily as base and surface material for logging roads. Flows of the Columbia River Basalt Group, especially the highly jointed entablatures, have more desirable engineering properties for most uses, and large quarries, all now abandoned, were developed in this unit southeast of Woodland. Abundant sand and gravel are available from unconsolidated alluvial deposits along the Lewis River.

## REFERENCES CITED


Allison, I.S., 1978, Late Pleistocene sediments and floods in the Willamette Valley: The Ore Bin, v. 40, p. 177–203.

Atwater, B.F., 1986, Pleistocene glacial-lake deposits of the Sanpoil River Valley, northeastern Washington: U.S. Geological Survey Bulletin 1661, 39 p.

Baker, V.R., and Bunker, R.C., 1985, Cataclysmic late Pleistocene flooding from glacial Lake Missoula—a review: Quaternary Science Reviews, v. 4, p. 1–41.

Balsillie, J.H., and Benson, G.T., 1971, Evidence for the Portland Hills Fault: The Ore Bin, v. 33, p. 109–118.

Barnosky, C.W., 1984, Late Pleistocene and early Holocene environmental history of southwestern Washington State, U.S.A.: Canadian Journal of Earth Sciences, v. 21, p. 619–629.

Bates, R.G., Beck, M.E., Jr., and Burmester, R.F., 1981, Tectonic rotations in the Cascade Range of southern Washington: Geology, v. 9, p. 184–189.

Beck, M.E., Jr., and Burr, C.D., 1979, Paleomagnetism and tectonic significance of the Goble Volcanic Series, southwestern Washington: Geology, v. 7, p. 175–179.

Beeson, M.H., Fecht, K.R., Reidel, S.P., and Tolan, T.L., 1985, Regional correlations within the Frenchman Springs Member of the Columbia River Basalt Group—new insights into the middle Miocene tectonics of northwestern Oregon: Oregon Geology, v. 47, p. 87–96.

Beeson, M.H., and Tolan, T.L., 1990, The Columbia River Basalt Group in the Cascade Range; a middle Miocene reference datum for structural analysis: Journal of Geophysical Research, v. 96, p. 19,547–19,559.

Beeson, M.H., Tolan, T.L., and Anderson, J. L., 1989, The Columbia River Basalt Group in western Oregon; geologic structures and other factors that controlled flow emplacement patterns, *in* Reidel, S.P., and Hooper, P.R, eds., Volcanism and tectonism in the Columbia River flood-basalt province: Geological Society of America Special Paper 239, p. 223–246.

Benito, G., and O'Connor, J.E., 2003, Number and size of last-glacial Missoula floods in the Columbia River valley between the Pasco Basin, Washington and Portland, Oregon: Geological Society of America Bulletin, v. 115, p. 624–638.

Berggren, W.A., Kent, D.V., Swisher, C., III, Aubry, M.-P., 1995, A revised Cenozoic geochronology and chronostratigraphy, *in* Berggren, W.A., Kent, D.V., Aubry, M.-P., and Hardenbol, Jan, eds., Geochronology,

time scales and global stratigraphic correlation: Society of Economic Paleontologists and Mineralogists Special Publication 54, p. 129–212.
Bet, J.N., and Rosner, M.L., 1993, Geology near Blue Lake County Park, eastern Multnomah County, Oregon: Oregon Geology, v. 55, p. 59–69.
Bjornstad, B.N., Fecht, K.R., and Pluhar, C.J., 2001, Long history of pre-Wisconsin, Ice Age cataclysmic floods—evidence from southeastern Washington State: Journal of Geology, v. 109, p. 695–713.
Blakely, R.J., Wells, R.E., Yelin, T.S., Madin, I.P., and Beeson, M.H., 1995, Tectonic setting of the Portland-Vancouver area, Oregon and Washington—constraints from low-altitude aeromagnetic data: Geological Society of America Bulletin, v. 107, p. 1051–1062.
Bott, J.D.J., and Wong, I.G., 1993, Historical earthquakes in and around Portland, Oregon: Oregon Geology, v. 55, p. 116–122.
Bretz, J H., 1925, The Spokane flood beyond the Channeled Scablands: Journal of Geology, v. 33, p. 97–115, p. 236–259.
Bretz, J H., 1959, Washington's Channeled Scabland: Washington Division of Mines and Geology Bulletin 45, 55 p.
Bretz, J H., Smith, H.T.U., and Neff, G.E., 1956, Channeled Scabland of Washington—new data and interpretations: Geological Society of America Bulletin, v. 67, p. 957–1049.
Byerly, G.R., and Swanson, D.A., 1987, The transition from subaerial to invasive lava flows, Grande Ronde Basalt, northwestern Columbia Plateau [abs.]: Geological Society of America Abstracts with Program, v. 19, p. 363.
Cas, R.A.F., and Wright, J.V., 1987, Volcanic successions—modern and ancient: London, Allen and Unwin, 528 p.
Cerling, T.E., Brown, F.H., and Bowman, J.R., 1985, Low-temperature alteration of volcanic glass—hydration, Na, K, $^{18}O$ and Ar mobility: Chemical Geology, v. 52, p. 281–293.
Cho, M., Maruyama, S., and Liou, J.G., 1987, An experimental investigation of heulandite-laumontite equilibrium at 1000 to 2000 bar $P_{\mathrm{fluid}}$: Contributions to Mineralogy and Petrology, v. 97, p. 43–50.
Clague, J.J., Barendregt, R., Enkin, R.J., and Foit, F.F., Jr., 2003, Paleomagnetic and tephra evidence for tens of Missoula floods in southern Washington: Geology, v. 31, p. 247–250.
Clark, P.U., and Mix, A.C., 2002, Ice sheets and sea level of the Last Glacial Maximum: Quaternary Science Reviews, v. 21, p. 1–7.
Colman, S.M., and Pierce, K.L., 1981, Weathering rinds on andesitic and basaltic stones as a Quaternary age indicator, western United States: U.S. Geological Survey Professional Paper 1210, 56 p.
Conrey, R.M., Sherrod, D.R., Uto, K., Uchiumi, S., 1996b, Potassium-argon ages from Mount Hood area of Cascade Range, northern Oregon: Isochron West, no. 63, p. 10–20.
Conrey, R.M., Uto, K., Uchiumi, S., Beeson, M.H., Madin, I.P., Tolan, T.L., and Swanson, D.A., 1996a, Potassium-argon ages of Boring Lava, northwest Oregon and southwest Washington: Isochron West, no. 63, p. 3–9.
Crandell, D.R., 1987, Deposits of pre-1980 pyroclastic flows and lahars from Mount St. Helens, Washington: U.S. Geological Survey Professional Paper 1444, 91 p.
Crandell, D.R., and Miller, R.D., 1974, Quaternary stratigraphy and extent of glaciation in the Mount Rainier region, Washington: U.S. Geological Survey Professional Paper 847, 59 p.
Dethier, D.P., 1988, The soil chronosequence along the Cowlitz River, Washington: U.S. Geological Survey Bulletin 1590-F, p. F1–F47.
Duncan, R.A., and Kulm, L.D., 1989, Plate tectonic evolution of the Cascades arc-subduction complex, *in* Winterer, E.L., Hussong, D.M., and Decker, R.W., eds., The eastern Pacific Ocean and Hawaii: Boulder, Colo., Geological Society of America, The geology of North America, v. N, p. 413–438.
Engebretson, D.C., Cox, A., and Gordon, R.G., 1985, Relative motions between oceanic and continental plates in the Pacific Basin: Geological Society of America Special Paper 206, 59 p.
Evarts, R.C., 2001, Geologic map of the Silver Lake quadrangle, Cowlitz County, Washington: U.S. Geological Survey Miscellaneous Field Studies Map MF-2371, scale 1:24,000, with 37-p. pamphlet [Available on the World Wide Web at http://geopubs.wr.usgs.gov/map-mf/mf2371/].
Evarts, R.C., 2002, Geologic map of the Deer Island quadrangle, Columbia County, Oregon and Cowlitz County, Washington: U.S. Geological Survey Miscellaneous Field Studies Map MF-2392, scale 1:24,000, with 33-p. pamphlet [Available on the World Wide Web at http://geopubs.wr.usgs.gov/map-mf/mf2392/].
Evarts, R.C., 2004, Geologic map of the Ariel quadrangle, Clark and Cowlitz Counties, Washington: U.S. Geological Survey Scientific Investigations Map 2826, scale 1:24,000, with 35-p. pamphlet [Available on the World Wide Web at http://pubs.usgs.gov/sim/2826].

Evarts, R.C., and Ashley, R.P., 1990a, Preliminary geologic map of the Cougar quadrangle, Cowlitz and Clark Counties, Washington: U.S. Geological Survey Open-File Report 90-631, scale 1:24,000, with 40-p. pamphlet.

Evarts, R.C., and Ashley, R.P., 1990b, Preliminary geologic map of the Goat Mountain quadrangle, Cowlitz County, Washington: U.S. Geological Survey Open-File Report 90-632, scale 1:24,000, with 47-p. pamphlet.

Evarts, R.C., and Ashley, R.P., 1991, Preliminary geologic map of the Lakeview Peak quadrangle, Cowlitz County, Washington: U.S. Geological Survey Open-File Report 91-289, scale 1:24,000, with 35-p. pamphlet.

Evarts, R.C., and Ashley, R.P., 1992, Preliminary geologic map of the Elk Mountain quadrangle, Cowlitz County, Washington: U.S. Geological Survey Open-File Report 92-362, scale 1:24,000, with 44-p. pamphlet.

Evarts, R.C., and Ashley, R.P., 1993, Geologic map of the Spirit Lake East quadrangle, Skamania County, Washington: U.S. Geological Survey Geologic Quadrangle Map GQ-1679, scale 1:24,000, with 12-p. pamphlet.

Evarts, R.C., Ashley, R.P., and Smith, J.G., 1987, Geology of the Mount St. Helens area—record of discontinuous volcanic and plutonic activity in the Cascade arc of southern Washington: Journal of Geophysical Research, v. 92, p. 10,155–10,169.

Evarts, R.C., and Bishop, K.R., 1994, Chemical data for Tertiary volcanic and intrusive rocks of the Spirit Lake 15-minute quadrangle, southern Washington Cascade Range: U.S. Geological Survey Open-File Report 93-686, 24 p.

Evarts, R.C., Clynne, M.A., Fleck, R.J., Lanphere, M.A., Calvert, A.T., and Sarna-Wojcicki, A.M., 2003, The antiquity of Mount St. Helens and age of the Hayden Creek Drift [abs.]: Geological Society of America Abstracts with program, v. 35, no. 6, p. 80.

Evarts, R.C., Hagstrum, J.T., Blakely, R.J., Dinterman, P.A., and Block, J.L., 2002, Complex right-lateral faulting at the northern end of the Portland Basin—geologic, aeromagnetic, and paleomagnetic evidence: Geological Society of America Abstracts with Programs, v. 34, no. 5, p.A33.

Evarts, R.C., and Swanson, D.A., 1994, Geologic transect across the Tertiary Cascade Range, southern Washington, *in* Swanson, D.A., and Haugerud, R.A., eds., Geologic field trips in the Pacific Northwest, 1994 Geological Society of America Meeting: Seattle, University of Washington Department of Geological Sciences, v. 2, p. 2H1–2H31.

Fiksdal, A.J., 1975, Slope stability of Clark County, Washington: Washington Division of Geology and Earth Resources Open-File Report 75-10, scale 1:62,500, with 4-p. pamphlet.

Fiske, R.S., Hopson, C.A., and Waters, A.C., 1963, Geology of Mount Rainier National Park, Washington: U.S. Geological Survey Professional Paper 444, 93 p.

Gates, E.B., 1994, The Holocene sedimentary framework of the lower Columbia River basin [MS thesis]: Portland, Oreg., Portland State University, 210 p.

Gill, J.B., 1981, Orogenic andesites and plate tectonics: New York, Springer-Verlag, 390 p.

Grant, A.R., 1969, Chemical and physical controls for base metal deposition in the Cascade Range of Washington: Washington Division of Mines and Geology Bulletin 58, 107 p.

Grigg, L.D., and Whitlock, C., 2002, Patterns and causes of millennial-scale climate change in the Pacific Northwest during Marine Isotope stages 2 and 3: Quaternary Science Reviews, v. 21, p. 2067–2083.

Hagstrum, J.T., Swanson, D.A., and Evarts, R.C., 1999, Paleomagnetism of an east-west transect across the Cascade arc in southern Washington—implications for regional tectonism: Journal of Geophysical Research, v. 104, p. 12853–12864.

Harp, E.L., Chleborad, A.F., Schuster, R.L., Cannon, S.H., Reid, M.E., and Wilson, R.C., 1997, Landslides and landslide hazards in Washington State due to February 5–9, 1996 storm: U.S. Geological Survey Administrative Report to the Federal Emergency Management Agency, 29 p.

Hill, B.E., and Taylor, E.M., 1989, Oregon Central High Cascade pyroclastic units in the vicinity of Bend, Oregon, *in* Scott, W.E., Gardner, C.A., and Sarna-Wojcicki, A.M., eds., Guidebook for field trip to the Mount Batchelor-South Sister-Bend area, Central Oregon High Cascades: U.S. Geological Survey Open-File Report 89-645, p. 51–54.

Hodge, E.T., 1938, Geology of the lower Columbia River: Geological Society of America Bulletin, v. 49, p. 836–929.

Hooper, P.R., 2000, Chemical discrimination of Columbia River Basalt flows: Geochemistry, Geophysics, Geosystems, v. 1, paper no. 2000GC000040 [www.g-cubed.org].

Howard, K.A., 2002, Geologic map of the Battle Ground 7.5-minute quadrangle, Clark County, Washington: U.S. Geological Survey Miscellaneous Field Studies Map MF-2395, scale 1:24,000, with 18-p. pamphlet [Available on the World Wide Web at http://geopubs.wr.usgs.gov/map-mf/mf2395/].

Johnson, D.M., Hooper, P.R., and Conrey, R.M., 1999, XRF analysis of rocks and minerals for major and trace elements on a single low dilution Li-tetraborate fused bead: Advances in X-ray Analysis, v. 41, p. 843–867.

Johnson, R.G., and King, B.-S., 1987, Energy-dispersive X-ray fluorescence spectrometry, *in* Baedecker, P.A., ed., Methods for geochemical analysis: U.S. Geological Survey Bulletin 1770, p. F1–F5.

King, B.-S., and Lindsay, J., 1990, Determination of 12 selected trace elements in geological materials by energy-dispersive X-ray fluorescence spectroscopy, *in* Arbogast, B.F., ed., Quality assurance manual for the Branch of Geochemistry, U.S. Geological Survey: U.S. Geological Survey Open-File Report 90-668, p. 161–165.

Lanphere, M.A., Champion, D.E., Christiansen, R.L., Donnelly-Nolan, J.M., Fleck, R.J., Sarna-Wojcicki, A.M., Obradovich, J.D., and Izett, G.A., 1999, Evolution of tephra dating in the western United States [abs.], Geological Society of America Abstracts with Program, v. 31, no. 6, p. A73.

Le Maitre, R.W., 2002, Igneous rocks—a classification and glossary of terms, 2d ed.: Cambridge University Press, 236 p.

Liberty, L.M., Hemphill-Haley, M.A., and Madin, I.P., 2003, The Portland Hills Fault—uncovering a hidden fault in Portland, Oregon, using high-resolution geophysical methods: Tectonophysics, v. 368, p. 89–103.

Livingston, V.E., Jr., 1966, Geology and mineral resources of Kelso-Cathlamet area, Cowlitz and Wahkiakum Counties, Washington: Washington Division of Mines and Geology Bulletin 54, 110 p.

Long, P.E., and Wood, B.J., 1986, Structures, textures, and cooling histories of Columbia River basalt flows: Geological Society of America Bulletin, v. 97, p. 1144–1155.

Lowry, W.D., and Baldwin, E.M., 1952, Late Cenozoic geology of the lower Columbia River valley, Oregon and Washington: Geological Society of America Bulletin, v. 63, p. 1–24.

Mabey, M.A., and Madin, I.P., 1995, Downhole and seismic cone penetrometer shear-wave velocity measurements for the Portland metropolitan area, 1993 and 1994: Oregon Department of Geology and Mineral Industries Open-File Report O-95-7, 69 p.

Madin, I.P., and Wang, Z., 1999, Relative earthquake hazard maps for selected urban areas in western Oregon—Dallas, Hood River, McMinnville-Dayton-Lafayette, Monmouth-Independence, Newberg-Dundee, Sandy, Sheridan-Willamina, Saint Helens-Columbia City-Scappoose: Oregon Department of Geology and Mineral Industries Interpretive Map Series Map IMS-7, scale 1:24,000, with 24-p. pamphlet.

Major, J.J., and Scott, K.M., 1988, Volcaniclastic sedimentation in the Lewis River valley, Mount St. Helens, Washington—processes, extent, and hazards: U.S. Geological Survey Bulletin 1383-D, 38 p.

Mangan, M.T., Wright, T.L., Swanson, D.A., and Byerly, G.R., 1986, Regional correlation of Grande Ronde Basalt flows, Columbia River Basalt Group, Washington, Oregon, and Idaho: Geological Society of America Bulletin, v. 97, p. 1300–1318.

McDonald, E.V., and Busacca, A.J., 1988, Record of pre-late Wisconsin giant floods in the Channeled Scabland interpreted from loess deposits: Geology, v. 16, p. 728–731.

Miall, A.D., 1977, A review of the braided river depositional environment: Earth-Science Reviews, v. 13, p. 1–62.

Miall, A.D., 1996, The geology of fluvial deposits—sedimentary facies, basin analysis, and petroleum geology: Berlin, Springer, 582 p.

Miyashiro, A., 1974, Volcanic rocks series in island arcs and active continental margins: American Journal of Science, v. 274, p. 321–355.

Mundorff, M.J., 1964, Geology and ground-water conditions of Clark County, Washington, with a description of a major alluvial aquifer along the Columbia River: U.S. Geological Survey Water-Supply Paper 1600, 268 p., scale 1:48,000.

Mundorff, M.J., 1984, Glaciation in the lower Lewis River basin, southwestern Cascade Range, Washington: Northwest Science, v. 58, p. 269–281.

Niem, A.R., MacLeod, N.S., Snavely, P.D., Jr., Huggins, D., Fortier, J.D., Meyer, H.J., Seeling, A., and Niem, W.A., 1992, Onshore-offshore geologic cross section, northern Oregon Coast Range to continental slope: Oregon Department of Geology and Mineral Industries Special Paper 26, scale 1:100,000.

Niem, A.R., McKnight, B.K., and Meyer, H.J., 1994, Sedimentary, volcanic, and tectonic framework of forearc basins and the Mist gas field, northwest Oregon, *in* Swanson, D.A., and Haugerud, R.A., eds., Geologic field trips in the Pacific Northwest, 1994 Geological Society of America Meeting: Seattle, University of Washington Department of Geological Sciences, v. 1, p. 1F1–1F42.

O'Connor, J.E., and Baker, V.R., 1992, Magnitudes and implications of peak discharges from glacial Lake Missoula: Geological Society of America Bulletin, v. 104, p. 267–279.

Orton, G.J., 1996, Volcanic environments, *in* Reading, H.G., ed., Sedimentary environments—processes, facies and stratigraphy (3d ed.): Oxford, Blackwell Science, Ltd., p. 485–567.

Pezzopane, S.K., and Weldon, R.J., II, 1993, Tectonic role of active faulting in central Oregon: Tectonics, v. 12, p. 1140–1169.

Phillips, W.M., 1987a, comp., Geologic map of the Vancouver quadrangle, Washington: Washington Division of Geology and Earth Resources Open-File Report 87-10, scale 1:100,000, with 27-p. pamphlet.

Phillips, W.M., 1987b, comp., Geologic map of the Mount St. Helens quadrangle, Washington: Washington Division of Geology and Earth Resources Open-File Report 87-04, scale 1:100,000, with 59-p. pamphlet.

Ramos, Amparo, and Sopeña, Alfonso, 1983, Gravel bars in low-sinuosity streams (Permian and Triassic, central Spain), *in* Collinson, J.D., and Lewin, J., Modern and ancient fluvial systems: International Association of Sedimentologists Special Publication No. 6, p. 301–312.

Reidel, S.P., 1998, Emplacement of Columbia River flood basalt: Journal of Geophysical Research, v. 103, p. 27,393–27,410.

Reidel, S.P., Tolan, T.L., Hooper, P.R., Beeson, M.H., Fecht, K.R., Bentley, R.D., and Anderson, J.L., 1989, The Grande Ronde Basalt, Columbia River Basalt Group; Stratigraphic descriptions and correlations in Washington, Oregon, and Idaho, *in* Reidel, S.P., and Hooper, P.R., eds., Volcanism and tectonism in the Columbia River flood-basalt province: Geological Society of America Special Paper 239, p. 21–53.

Roberts, A.E., 1958, Geology and coal resources of the Toledo-Castle Rock district, Cowlitz and Lewis Counties, Washington: U.S. Geological Survey Bulletin 1062, 71 p.

Rust, B.R., 1978, Depositional models for braided alluvium, *in* Miall, A.D., ed., Fluvial sedimentology: Canadian Society of Petroleum Geologists Memoir 5, p. 605–625.

Sarna-Wojcicki, A.M., Meyer, C.E. Nakata, J.K., Scott, W.E., Hill, B.E., Slate, J.L., and Russell, P.C., 1989, Age and correlation of mid-Quaternary ash beds and tuffs in the vicinity of Bend, Oregon, *in* Scott, W.E., Gardner, C.A., and Sarna-Wojcicki, A.M., eds., Guidebook for field trip to the Mount Bachelor-South Sister-Bend area, central Oregon High Cascades: U.S. Geological Survey Open-File Report 89-645, p. 55–62.

Smith, G.A., 1986, Coarse-grained nonmarine volcaniclastic sediment—terminology and depositional processes: Geological Society of America Bulletin, v. 97, p. 1–10.

Smith, G.A., 1988, Neogene synvolcanic and syntectonic sedimentation in central Washington: Geological Society of America Bulletin, v. 100, p. 1479–1492.

Smith, J.G., 1993, Geologic map of upper Eocene to Holocene volcanic and related rocks in the Cascade Range, Washington: U.S. Geological Survey Miscellaneous Investigations Series Map I-2005, scale 1:500,000.

Snavely, P.D., Jr., MacLeod, N.S., and Wagner, H.C., 1973, Miocene tholeiitic basalts of coastal Oregon and Washington and their relations to coeval basalts of the Columbia Plateau: Geological Society of America Bulletin, v. 84, p. 387–424.

Snavely, P.D., Jr., and Wells, R.E., 1996, Cenozoic evolution of the continental margin of Oregon and Washington, *in* Rogers, A.M., Walsh, T.J., Kockelman, W.J., and Priest, G.R., eds., Assessing earthquake hazards and reducing risk in the Pacific Northwest: U.S. Geological Survey Professional Paper 1560, p. 161–182.

Swanson, D.A., Wright, T.L., Hooper, P.R., Bentley, R.D., 1979, Revisions in stratigraphic nomenclature of the Columbia River Basalt Group: U.S. Geological Survey Bulletin 1457-G, 59 p.

Swanson, R.D., 1986, A stratigraphic-geochemical study of the Troutdale Formation and Sandy River Mudstone in the Portland basin and lower Columbia River Gorge [MS thesis]: Portland, Oreg., Portland State University, 103 p.

Swanson, R.D., McFarland, W.D., Gonthier, J.B., and Wilkinson, J.M., 1993, A description of hydrogeologic units in the Portland Basin, Oregon and Washington: U.S. Geological Survey Water-Resources Investigations Report 90-4196, 56 p., scale 1:100,000.

Taggart, J.E., Jr., Lindsay, J.R., Scott, B.A., Vivit, D.V., Bartel, A.J., and Stewart, K.C., 1987, Analysis of geological materials by wavelength-dispersive X-ray fluorescence spectrometry, *in* Baedecker, P.A., ed., Methods for geochemical analysis: U.S. Geological Survey Bulletin 1770, p. E1–E19.

Tolan T.L., and Beeson, M.H., 1984, Intracanyon flows of the Columbia River Basalt group in the lower Columbia River Gorge and their relationship to the Troutdale Formation: Geological Society of America Bulletin, v. 95, p. 463–477.

Tolan T.L., and Beeson, M.H., 1999, Geologic map of the Scotts Mills, Silverton, and Slayton Northeast 7.5-minute quadrangles, Oregon: U.S. Geological Survey Open-File Report 99-141, scale 1:24,000.

Tolan, T.L., Reidel, S.P., Beeson, M.H., Anderson, J.L., Fecht, K.R., and Swanson, D.A., 1989, Revisions to the estimates of the areal extent and volume of the Columbia River Basalt Group, *in* Reidel, S.P., and Hooper, P.R, eds., Volcanism and tectonism in the Columbia River flood-basalt province: Geological Society of America Special Paper 239, p. 1–20.

Trimble, D.E., 1957, Geology of the Portland quadrangle, Oregon-Washington: U.S. Geological Survey Geologic Quadrangle Map GQ-104, scale 1:62,500.

Trimble, D.E., 1963, Geology of Portland, Oregon and adjacent areas: U.S. Geological Survey Bulletin 1119, 119 p., scale 1:62,500.

Van Atta, R.O., and Kelty, K.B., 1985, Scappoose Formation, Columbia County, Oregon—new evidence of age and relation to Columbia River Basalt Group: American Association of Petroleum Geologists Bulletin, v. 69, p. 688–698.

Verplanck, E.P., and Duncan, R.A., 1987, Temporal variations in plate convergence and eruption rates in the Western Cascades, Oregon: Tectonics, v. 6, p. 197–209.

Vessell, R.K., and Davies, D.K., 1981, Nonmarine sedimentation in an active fore arc basin, *in* Ethridge, F.G., and Flores, R.M., eds., Recent and ancient nonmarine depositional environments—models for exploration: Society of Economic Paleontologists and Mineralogists Special Publication 31, p. 31–45.

Waitt, R.B., Jr., 1985, Case for periodic, colossal jökulhlaups from Pleistocene glacial Lake Missoula: Geological Society of America, v. 96, p. 1271–1286.

Waitt, R.B., Jr., 1994, Scores of gigantic, successively smaller Lake Missoula floods through channeled scabland and Columbia valley, *in* Swanson, D.A., and Haugerud, R.A., eds., Geologic field trips in the Pacific Northwest: Seattle, University of Washington Department of Geological Sciences, p. 1K1–1K88.

Waitt, R.B., Jr., 1996, Numerous colossal Missoula Floods through Columbia Gorge and Portland-Vancouver basin [abs.]: Geological Society of America Abstracts with Program, v. 28, no. 5, p. 120–121.

Walsh, T.J., Korosec, M.A., Phillips, W.M., Logan, R.L., and Schasse, H.W., 1987, Geologic map of Washington—southwest quadrant: Washington Division of Geology and Earth Resources Map GM-34, scale 1:250,000.

Warne, A.G., and Stanley, D.J., 1995, Sea-level changes as critical factor in development of basin margin sequences—new evidence from late Quaternary record: Journal of Coastal Research Special Issue 17, p. 231–240.

Wegmann, K.W., and Walsh, T.J., 2001, Landslide hazards mapping in Cowlitz County—a progress report: Washington Geology, v. 29, no. 1/2, p. 30–33.

Wells, R.E., 1981, Geologic map of the eastern Willapa Hills, Cowlitz, Lewis, Pacific, and Wahkiakum Counties, Washington: U.S. Geological Survey Open-File Report 81-674, scale 1:62,500.

Wells, R.E., 1989, Mechanisms of Cenozoic tectonic rotation, Pacific Northwest convergent margin, U.S.A., *in* Kissel, Catherine, and Laj, Carol, eds., Paleomagnetic rotations and continental deformation: Dordrecht, Kluwer Academic Publishers, p. 313–325.

Wells, R.E., 1990, Paleomagnetic rotations and the Cenozoic tectonics of the Cascade arc, Washington, Oregon, and California: Journal of Geophysical Research, v. 95, p. 19,409–19,417.

Wells, R.E., and Coe, R.S., 1985, Paleomagnetism and geology of Eocene volcanic rocks of southwest Washington, implications for mechanisms of tectonic rotation: Journal of Geophysical Research, v. 90, p. 1925–1947.

Wells, R.E., and Niem, A.R., 1987, Geology of the Columbia River Basalt in the Astoria Basin, Oregon and Washington [abs.]: Geological Society of America Abstracts with Program, v. 19, p. 462–463.

Wells, R.E., Simpson, R.W., Bentley, R.D., Beeson, M.H., Mangan, M.T., and Wright, T.L., 1989, Correlation of Miocene flows of the Columbia River Basalt Group from the central Columbia River Plateau to the coast of Oregon and Washington, *in* Reidel, S.P., and Hooper, P.R., eds., Volcanism and tectonism in the Columbia River flood-basalt province: Geological Society of America Special Paper 239, p. 113–129.

Wells, R.E., Weaver, C.S., and Blakely, R.J., 1998, Fore-arc migration in Cascadia and its neotectonic significance: Geology, v. 26, p. 759–762.

Whetten, J.T., Kelley, J.C., and Hanson, L.G., 1969, Characteristics of Columbia River sediment and sediment transport: Journal of Sedimentary Petrology, v. 39, p. 1149–1166.

Wilkinson, W.D., Lowry, W.D., and Baldwin, E.M., 1946, Geology of the St. Helens quadrangle, Oregon: Oregon Department of Geology and Mineral Industries Bulletin 31, 39 p., scale 1:62,500.

Williams, H., and McBirney, A.R., 1979, Volcanology: San Francisco, Freeman, Cooper and Co., 397 p.

Wise, W.S., 1970, Cenozoic volcanism in the Cascade Mountains of southern Washington: Washington Division of Mines and Geology Bulletin 60, 45 p.

Wolfe, J.A., 1978, A paleobotanical interpretation of Tertiary climates in the Northern Hemisphere: American Scientist, v. 66, p. 694–703.

Wolfe, J.A., and Hopkins, D.M., 1967, Climatic changes recorded by Tertiary land floras in northwestern North America, *in* Hatai, Kotora, ed., Tertiary correlations and climatic changes in the Pacific: Sendai, Japan, Sendai Printing and Publishing, p. 67–76.

Wong, I.G., Hemphill-Haley, A., Liberty, L.M., and Madin, I.P., 2001, The Portland Hills Fault—an earthquake generator or just another old fault?: Oregon Geology, v. 63, p. 39–50.

Yeats, R.S., Graven, E.P., Werner, K.S., Goldfinger, Chris, and Popowski, T.A., 1996, Tectonics of the Willamette Valley, Oregon, *in* Rogers, A.M., Walsh, T.J., Kockelman, W.J., and Priest, G.R., eds., Assessing earthquake hazards and reducing risk in the Pacific Northwest: U.S. Geological Survey Professional Paper 1650, v. 1, p. 183–222.

Yelin, T.S., and Patton, H.J., 1991, Seismotectonics of the Portland, Oregon, region: Seismological Society of America Bulletin, v. 81, p. 109–130.

Zuffa, G.G., Normark, W.R., Serra, F., and Brunner, C.A., 2000, Turbidite megabeds in an oceanic rift valley recording jökulhlaups of late Pleistocene glacial lakes of the western United States: Journal of Geology, v. 108, p. 253–274.

**Table 1.** Chemical analyses and modes of volcanic and intrusive rocks, Woodland 7.5' quadrangle

[X-ray fluorescence analyses. Rock-type names assigned in accordance with IUGS system (Le Maitre, 2002) applied to recalculated analyses. LOI, loss on ignition. Mg#, atomic ratio 100Mg/(Mg+$Fe^{2+}$) with $Fe^{2+}$ set to 0.85x $Fe^{total}$. Modal analyses, secondary minerals counted as primary mineral replaced; -, not present. ---, no data. Analyses by D.F. Siems at U.S. Geological Survey, Lakewood, Colo. using methods described in Taggart and others (1987), Johnson and King (1987), and King and Lindsay (1990). *, analyses by D.M. Johnson at GeoAnalytical Laboratory of Washington State University using methods described in Johnson and others (1999)]

| Map No. | 1 | 2 | 3 | 4 | 5 | 6 | 7 | 8 | 9 |
|---|---|---|---|---|---|---|---|---|---|
| Field sample No. | 97LC-Q87 | 97LC-Q30A | 97LC-Q85A | 97LC-Q24 | 97LC-Q154 | 97LC-Q146 | 97LC-Q143s | 97LC-Q111 | 97LC-Q84A |
| Latitude (N) | 45°59.66' | 45°56.94' | 45°59.49' | 45°56.98' | 45°57.61' | 45°57.08' | 45°57.46' | 45°57.26' | 45°59.82' |
| Longitude (W) | 122°42.73' | 122°42.01' | 122°44.42' | 122°41.75' | 122°44.65' | 122°43.76' | 122°43.96' | 122°41.38' | 122°44.38' |
| Map unit | Tob | Tba | Tba | Tba | Tba | Tba | Tba | Tba | Tba |
| Rock type | Basalt | Basalt | Basalt | Basaltic andesite | Basaltic andesite | Basaltic andesite | Basaltic andesite | Basaltic andesite | Basaltic andesite |
| Analyses as reported (wt percent) | | | | | | | | | |
| $SiO_2$ | 49.97 | 49.93 | 50.36 | 50.68 | 52.27 | 51.52 | 51.46 | 51.83 | 52.55 |
| $TiO_2$ | 0.88 | 1.79 | 0.85 | 1.79 | 0.93 | 0.84 | 1.07 | 1.11 | 0.97 |
| $Al_2O_3$ | 16.08 | 16.11 | 16.92 | 16.08 | 17.50 | 17.41 | 16.67 | 16.97 | 18.64 |
| $Fe_2O_3$ | 8.48 | 10.91 | 9.08 | 10.74 | 9.08 | 7.94 | 8.50 | 8.40 | 8.27 |
| FeO | --- | --- | --- | --- | --- | --- | --- | --- | --- |
| MnO | 0.13 | 0.17 | 0.14 | 0.17 | 0.14 | 0.14 | 0.17 | 0.14 | 0.12 |
| MgO | 9.18 | 5.63 | 8.44 | 5.42 | 6.07 | 6.96 | 6.50 | 6.29 | 4.59 |
| CaO | 10.52 | 9.91 | 10.12 | 9.91 | 10.05 | 9.95 | 10.06 | 10.26 | 10.12 |
| $Na_2O$ | 2.55 | 2.90 | 2.47 | 2.81 | 2.71 | 2.47 | 2.48 | 2.52 | 2.94 |
| $K_2O$ | 0.79 | 0.59 | 0.46 | 0.55 | 0.51 | 0.44 | 0.61 | 0.48 | 0.47 |
| $P_2O_5$ | 0.23 | 0.39 | 0.19 | 0.39 | 0.16 | 0.17 | 0.20 | 0.22 | 0.15 |
| LOI | 0.99 | 1.33 | 1.00 | 1.49 | 0.98 | 2.29 | 2.34 | 1.78 | 1.29 |
| Total | 99.80 | 99.66 | 100.03 | 100.02 | 100.38 | 100.13 | 100.06 | 100.00 | 100.12 |
| Analyses recalculated volatile-free and normalized to 100% with all Fe as FeO (wt percent) | | | | | | | | | |
| $SiO_2$ | 51.01 | 51.35 | 51.33 | 52.00 | 53.07 | 53.08 | 53.12 | 53.22 | 53.62 |
| $TiO_2$ | 0.90 | 1.84 | 0.86 | 1.83 | 0.94 | 0.86 | 1.10 | 1.14 | 0.99 |
| $Al_2O_3$ | 16.41 | 16.57 | 17.24 | 16.50 | 17.77 | 17.94 | 17.21 | 17.43 | 19.02 |
| FeO* | 7.78 | 10.10 | 8.32 | 9.91 | 8.30 | 7.36 | 7.90 | 7.76 | 7.59 |
| MnO | 0.13 | 0.18 | 0.15 | 0.17 | 0.14 | 0.14 | 0.18 | 0.14 | 0.12 |
| MgO | 9.37 | 5.79 | 8.61 | 5.56 | 6.16 | 7.17 | 6.71 | 6.46 | 4.68 |
| CaO | 10.74 | 10.19 | 10.31 | 10.17 | 10.20 | 10.26 | 10.39 | 10.53 | 10.33 |
| $Na_2O$ | 2.60 | 2.98 | 2.51 | 2.89 | 2.75 | 2.55 | 2.56 | 2.59 | 3.00 |
| $K_2O$ | 0.81 | 0.60 | 0.47 | 0.56 | 0.51 | 0.46 | 0.63 | 0.49 | 0.48 |
| $P_2O_5$ | 0.23 | 0.40 | 0.19 | 0.40 | 0.16 | 0.18 | 0.21 | 0.23 | 0.15 |
| Mg# | 71.6 | 54.6 | 68.4 | 54.0 | 60.9 | 67.1 | 64.1 | 63.6 | 56.4 |
| Modes (volume percent) | | | | | | | | | |
| Plagioclase | 5.3 | 0.6 | 14.5 | - | 14.4 | 26.7 | 19.0 | 17.6 | 19.5 |
| Clinopyroxene | 3.8 | - | 6.1 | - | 0.1 | 0.5 | 3.7 | 3.3 | trace |
| Orthopyroxene | - | - | - | - | - | 0.2 | - | - | - |
| Olivine | 9.5 | 0.1 | 6.5 | - | 2.8 | 3.1 | 5.9 | 3.3 | 0.3 |
| Fe-Ti Oxide | trace | - | trace | - | trace | - | - | - | - |
| Hornblende | - | - | - | - | - | - | - | - | - |
| Quartz | - | - | - | - | - | - | - | - | - |
| K-feldspar | - | - | - | - | - | - | - | - | - |
| Other | - | - | - | - | - | - | - | - | - |
| Groundmass | 81.4 | 99.3 | 72.9 | 100.0 | 82.7 | 69.5 | 71.4 | 75.8 | 80.2 |
| No. points counted | 793 | 775 | 771 | --- | 796 | 765 | 783 | 788 | 814 |
| Texture (rock/ groundmass) | seriate/ intergranular | sparsely phyric/ trachytic | porphyritic/ intergranular | microphyric/ intergranular | porphyritic/ intergranular | seriate/ intergranular | seriate/ intersertal | porphyritic/ intergranular | porphyritic/ trachytic |
| Trace element analyses (ppm) | | | | | | | | | |
| Ba | 210 | 153 | 102 | 141 | 105 | 117 | 143 | 225 | 106 |
| Rb | 17 | 11 | 10 | 21 | 10 | <10 | 16 | 12 | <10 |
| Sr | 707 | 425 | 376 | 484 | 374 | 410 | 422 | 612 | 368 |
| Y | 15 | 29 | 14 | 24 | 16 | 13 | 16 | 15 | 15 |
| Zr | 107 | 189 | 94 | 188 | 79 | 108 | 124 | 140 | 83 |
| Nb | <10 | 20 | 10 | 16 | 10 | <10 | <10 | 10 | <10 |
| Ni | --- | --- | --- | --- | --- | --- | --- | --- | --- |
| Cu | --- | --- | --- | --- | --- | --- | --- | --- | --- |
| Zn | --- | --- | --- | --- | --- | --- | --- | --- | --- |
| Cr | --- | --- | --- | --- | --- | --- | --- | --- | --- |

**Table 1.** Chemical analyses of volcanic and intrusive rocks, Woodland 7.5' quadrangle—Continued

| Map No. | 10 | 11 | 12 | 13 | 14 | 15 | 16 | 17 | 18 |
|---|---|---|---|---|---|---|---|---|---|
| Field sample No. | 98LC-Q239 | 97LC-Q137A | 97LC-Q103B | 97LC-Q91 | 97LC-Q102C | 97LC-Q155B | 97LC-Q86A | 98LC-Q195 | 97LC-Q37 |
| Latitude (N) | 45°58.67' | 45°57.32' | 45°57.89' | 45°59.24' | 45°58.33' | 45°56.95' | 45°59.50' | 45°59.48' | 45°57.19' |
| Longitude (W) | 122°40.37' | 122°42.22' | 122°40.88' | 122°42.16' | 122°41.36' | 122°44.55' | 122°42.64' | 122°37.87' | 122°43.04' |
| Map unit | Tba | Tba | Tba | Tba | Tba | Tba | Tba | Tba | Tba |
| Rock type | Basaltic andesite | Basaltic andesite | Basaltic andesite | Basaltic andesite | Basaltic andesite | Basaltic andesite | Basaltic andesite | Basaltic andesite | Basaltic andesite |
| Analyses as reported (wt percent) | | | | | | | | | |
| $SiO_2$ | 52.26 | 52.23 | 52.85 | 53.21 | 52.83 | 52.96 | 53.50 | 53.11 | 53.39 |
| $TiO_2$ | 1.01 | 1.28 | 0.83 | 1.33 | 1.07 | 1.08 | 0.95 | 1.06 | 1.28 |
| $Al_2O_3$ | 16.66 | 17.18 | 17.75 | 17.76 | 17.25 | 17.40 | 18.27 | 17.53 | 16.76 |
| $Fe_2O_3$ | 9.05 | 9.22 | 7.79 | 9.72 | 8.63 | 8.91 | 8.44 | 8.67 | 8.87 |
| FeO | --- | --- | --- | --- | --- | --- | --- | --- | --- |
| MnO | 0.15 | 0.14 | 0.14 | 0.15 | 0.17 | 0.16 | 0.14 | 0.15 | 0.16 |
| MgO | 6.46 | 4.90 | 5.94 | 3.80 | 5.56 | 5.20 | 4.62 | 5.33 | 5.02 |
| CaO | 9.20 | 9.00 | 9.82 | 9.04 | 9.11 | 8.80 | 9.74 | 9.09 | 9.13 |
| $Na_2O$ | 2.70 | 3.11 | 2.69 | 3.44 | 3.04 | 3.16 | 3.13 | 3.05 | 3.10 |
| $K_2O$ | 0.51 | 0.74 | 0.62 | 0.61 | 0.38 | 0.63 | 0.49 | 0.29 | 0.66 |
| $P_2O_5$ | 0.16 | 0.26 | 0.19 | 0.22 | 0.23 | 0.21 | 0.16 | 0.21 | 0.27 |
| LOI | 1.48 | 1.90 | 1.70 | 0.91 | 1.71 | 1.40 | 0.68 | 1.39 | 0.79 |
| Total | 99.64 | 99.96 | 100.31 | 100.19 | 99.98 | 99.92 | 100.12 | 99.88 | 99.42 |
| Analyses recalculated volatile-free and normalized to 100% with all Fe as FeO (wt percent) | | | | | | | | | |
| $SiO_2$ | 53.74 | 53.77 | 54.02 | 54.13 | 54.24 | 54.25 | 54.27 | 54.41 | 54.62 |
| $TiO_2$ | 1.04 | 1.32 | 0.85 | 1.35 | 1.10 | 1.10 | 0.96 | 1.08 | 1.31 |
| $Al_2O_3$ | 17.13 | 17.69 | 18.14 | 18.06 | 17.71 | 17.83 | 18.53 | 17.95 | 17.14 |
| FeO* | 8.37 | 8.54 | 7.16 | 8.90 | 7.97 | 8.21 | 7.71 | 7.99 | 8.17 |
| MnO | 0.15 | 0.14 | 0.14 | 0.15 | 0.17 | 0.16 | 0.14 | 0.15 | 0.16 |
| MgO | 6.64 | 5.05 | 6.07 | 3.87 | 5.71 | 5.33 | 4.69 | 5.46 | 5.14 |
| CaO | 9.46 | 9.27 | 10.03 | 9.19 | 9.35 | 9.02 | 9.87 | 9.31 | 9.34 |
| $Na_2O$ | 2.77 | 3.20 | 2.75 | 3.50 | 3.12 | 3.24 | 3.18 | 3.13 | 3.17 |
| $K_2O$ | 0.53 | 0.76 | 0.63 | 0.62 | 0.39 | 0.65 | 0.50 | 0.30 | 0.67 |
| $P_2O_5$ | 0.17 | 0.27 | 0.19 | 0.22 | 0.24 | 0.22 | 0.16 | 0.22 | 0.28 |
| Mg# | 62.4 | 55.3 | 64.0 | 47.7 | 60.0 | 57.6 | 56.1 | 58.9 | 56.9 |
| Modes (volume percent) | | | | | | | | | |
| Plagioclase | 9.5 | 4.1 | 13.7 | 22.2 | 10.4 | 10.4 | 14.1 | 19.4 | 1.0 |
| Clinopyroxene | 0.1 | - | 0.2 | 0.8 | 0.2 | trace | trace | - | - |
| Orthopyroxene | - | - | - | - | - | - | - | - | - |
| Olivine | 4.4 | 0.1 | 2.7 | 0.2 | 1.9 | 0.9 | 0.8 | 2.3 | 0.4 |
| Fe-Ti Oxide | - | - | - | - | - | - | - | - | - |
| Hornblende | - | - | - | - | - | - | - | - | - |
| Quartz | - | - | - | - | - | - | - | - | - |
| K-feldspar | - | - | - | - | - | - | - | - | - |
| Other | - | - | - | - | - | - | - | - | - |
| Groundmass | 86.0 | 95.8 | 83.4 | 76.8 | 87.5 | 88.7 | 85.1 | 78.3 | 98.6 |
| No. points counted | 814 | 750 | 797 | 788 | 740 | 781 | 798 | 814 | 764 |
| Texture (rock/ groundmass) | seriate/ trachytic | porphyritic/ trachytic | seriate/ intergranular | seriate/ intergranular | porphyritic/ trachytic | seriate/ trachytic | porphyritic/ intergranular | seriate/ intergranular | sparsely phyric/ trachytic |
| Trace element analyses (ppm) | | | | | | | | | |
| Ba | 148 | 137 | 147 | 153 | 147 | 137 | 120 | 203 | 155 |
| Rb | 10 | 13 | 14 | 10 | 11 | <10 | 10 | 10 | 13 |
| Sr | 380 | 347 | 400 | 405 | 379 | 383 | 371 | 444 | 363 |
| Y | 16 | 21 | 17 | 16 | 18 | 18 | 15 | 17 | 21 |
| Zr | 89 | 151 | 130 | 115 | 133 | 111 | 83 | 133 | 158 |
| Nb | <10 | 11 | 11 | 10 | 12 | 10 | <10 | 13 | 15 |
| Ni | 114 | --- | --- | --- | --- | --- | --- | 62 | --- |
| Cu | 115 | --- | --- | --- | --- | --- | --- | 115 | --- |
| Zn | 75 | --- | --- | --- | --- | --- | --- | 77 | --- |
| Cr | --- | --- | --- | --- | --- | --- | --- | --- | --- |

**Table 1.** Chemical analyses of volcanic and intrusive rocks, Woodland 7.5' quadrangle—Continued

| Map No. | 19 | 20 | 21 | 22 | 23 | 24 | 25 | 26 | 27 |
|---|---|---|---|---|---|---|---|---|---|
| Field sample No. | 97LC-Q82 | 97LC-Q79 | 97LC-Q83 | 97LC-Q94 | 97LC-Q75 | 98LC-Q197A | 98LC-Q170 | 97LC-Q12 | 98LC-Q178 |
| Latitude (N) | 45°58.96' | 45°59.11' | 45°58.66' | 45°59.63' | 45°53.20' | 45°57.51' | 45°56.46' | 45°58.53' | 45°54.75' |
| Longitude (W) | 122°43.85' | 122°44.48' | 122°43.15' | 122°41.35' | 122°40.65' | 122°40.52' | 122°45.00' | 122°37.90' | 122°43.12' |
| Map unit | Tba | Tba | Tba | Tba | Tba | Tba | Tbb | Thba | Ta |
| Rock type | Basaltic andesite | Basaltic andesite | Basaltic andesite | Basaltic andesite | Basaltic andesite | Basaltic andesite | Basaltic andesite breccia | Hypersthene basaltic andesite | Andesite |
| Analyses as reported (wt percent) | | | | | | | | | |
| $SiO_2$ | 53.62 | 53.72 | 53.98 | 54.20 | 53.93 | 54.45 | 51.98 | 55.11 | 55.74 |
| $TiO_2$ | 1.13 | 1.39 | 1.21 | 1.16 | 1.21 | 1.27 | 1.30 | 0.82 | 1.36 |
| $Al_2O_3$ | 17.81 | 17.12 | 17.87 | 18.61 | 17.39 | 16.57 | 17.04 | 18.53 | 16.48 |
| $Fe_2O_3$ | 8.43 | 9.13 | 8.44 | 8.05 | 8.22 | 8.64 | 8.70 | 7.38 | 8.12 |
| FeO | --- | --- | --- | --- | --- | --- | --- | --- | --- |
| MnO | 0.15 | 0.15 | 0.14 | 0.15 | 0.16 | 0.14 | 0.16 | 0.12 | 0.14 |
| MgO | 4.78 | 4.22 | 3.79 | 3.48 | 3.98 | 4.35 | 5.47 | 4.16 | 2.91 |
| CaO | 9.20 | 9.24 | 9.07 | 9.10 | 9.17 | 8.74 | 9.12 | 8.16 | 7.63 |
| $Na_2O$ | 3.15 | 3.26 | 3.29 | 3.24 | 2.99 | 3.20 | 2.88 | 3.14 | 3.43 |
| $K_2O$ | 0.52 | 0.49 | 0.75 | 0.65 | 0.72 | 0.84 | 0.45 | 0.97 | 0.64 |
| $P_2O_5$ | 0.20 | 0.29 | 0.23 | 0.21 | 0.26 | 0.27 | 0.26 | 0.17 | 0.38 |
| LOI | 1.25 | 1.06 | 1.15 | 1.07 | 1.96 | 1.15 | 2.17 | 1.36 | 2.77 |
| Total | 100.23 | 100.05 | 99.91 | 99.92 | 99.99 | 99.61 | 99.53 | 99.92 | 99.61 |
| Analyses recalculated volatile-free and normalized to 100% with all Fe as FeO (wt percent) | | | | | | | | | |
| $SiO_2$ | 54.64 | 54.77 | 55.13 | 55.28 | 55.49 | 55.80 | 53.87 | 56.34 | 58.05 |
| $TiO_2$ | 1.15 | 1.41 | 1.23 | 1.18 | 1.24 | 1.30 | 1.34 | 0.84 | 1.42 |
| $Al_2O_3$ | 18.15 | 17.45 | 18.25 | 18.99 | 17.89 | 16.97 | 17.66 | 18.94 | 17.16 |
| FeO* | 7.73 | 8.38 | 7.75 | 7.39 | 7.61 | 7.96 | 8.12 | 6.78 | 7.61 |
| MnO | 0.15 | 0.15 | 0.15 | 0.15 | 0.16 | 0.15 | 0.16 | 0.12 | 0.14 |
| MgO | 4.87 | 4.30 | 3.87 | 3.54 | 4.09 | 4.46 | 5.67 | 4.25 | 3.03 |
| CaO | 9.37 | 9.42 | 9.26 | 9.28 | 9.43 | 8.96 | 9.45 | 8.35 | 7.95 |
| $Na_2O$ | 3.21 | 3.32 | 3.36 | 3.30 | 3.08 | 3.28 | 2.99 | 3.21 | 3.57 |
| $K_2O$ | 0.53 | 0.49 | 0.77 | 0.67 | 0.74 | 0.86 | 0.47 | 0.99 | 0.67 |
| $P_2O_5$ | 0.20 | 0.30 | 0.23 | 0.21 | 0.27 | 0.27 | 0.27 | 0.17 | 0.40 |
| Mg# | 56.9 | 51.8 | 51.1 | 50.2 | 53.0 | 54.0 | 59.4 | 56.8 | 45.5 |
| Modes (volume percent) | | | | | | | | | |
| Plagioclase | 32.9 | 17.4 | 15.5 | 21.2 | 20.4 | - | 3.9 | 34.9 | 18.7 |
| Clinopyroxene | 0.5 | 0.6 | 0.1 | 0.3 | 0.5 | - | - | 0.3 | 0.7 |
| Orthopyroxene | 2.9 | - | - | - | - | - | - | 7.3 | 0.4 |
| Olivine | 1.4 | 0.3 | 0.3 | 0.7 | 0.3 | - | 0.3 | - | 0.5 |
| Fe-Ti Oxide | - | - | - | - | - | - | - | - | 0.1 |
| Hornblende | - | - | - | - | - | - | - | - | - |
| Quartz | - | - | - | - | - | - | - | - | - |
| K-feldspar | - | - | - | - | - | - | - | - | - |
| Other | - | - | - | - | - | - | - | - | - |
| Groundmass | 62.3 | 81.7 | 84.1 | 77.8 | 78.8 | 100.0 | 95.8 | 57.5 | 79.6 |
| No. points counted | 750 | 791 | 780 | 776 | 814 | --- | 755 | 800 | 791 |
| Texture (rock/ groundmass) | seriate/ intergranular | seriate/ trachytic | glomerophyric/ intergranular | seriate/ intergranular | porphyritic/ intersertal | aphyric/ trachytic | seriate/ subophitic | porphyritic/ intergranular | porphyritic/ hyalopilitic |
| Trace element analyses (ppm) | | | | | | | | | |
| Ba | 128 | 164 | 163 | 125 | 269 | 186 | 258 | 149 | 238 |
| Rb | <10 | 12 | 16 | <10 | 43 | 15 | 11 | 17 | 24 |
| Sr | 412 | 405 | 426 | 414 | 388 | 360 | 356 | 427 | 411 |
| Y | 18 | 18 | 19 | 14 | 21 | 26 | 27 | 17 | 31 |
| Zr | 112 | 136 | 129 | 122 | 157 | 161 | 147 | 138 | 236 |
| Nb | 10 | 10 | <10 | 12 | 12 | 15 | 10 | 12 | 15 |
| Ni | --- | --- | --- | --- | --- | 34 | 56 | --- | 12 |
| Cu | --- | --- | --- | --- | --- | 77 | 89 | --- | 111 |
| Zn | --- | --- | --- | --- | --- | 72 | 91 | --- | 87 |
| Cr | --- | --- | --- | --- | --- | --- | --- | --- | --- |

**Table 1.** Chemical analyses of volcanic and intrusive rocks, Woodland 7.5' quadrangle—Continued

| Map No. | 28 | 29 | 30 | 31 | 32 | 33 | 34 | 35 | 36 |
|---|---|---|---|---|---|---|---|---|---|
| Field sample No. | 97LC-Q54 | 97LC-Q80 | 97LC-Q71C | 98LC-Q259A | 97LC-Q07 | 97LC-Q33 | 97LC-Q109 | 98LC-Q177 | 97LC-Q76 |
| Latitude (N) | 45°54.74' | 45°58.68' | 45°53.14' | 45°52.90' | 45°58.02' | 45°58.25' | 45°57.85' | 45°54.69' | 45°54.48' |
| Longitude (W) | 122°41.57' | 122°44.05' | 122°40.30' | 122°40.91' | 122°39.67' | 122°42.48' | 122°39.20' | 122°40.21' | 122°41.88' |
| Map unit | Ta | Ta | Ta | Ta | Ta | Ta | Td | Td | Td |
| Rock type | Andesite | Andesite | Andesite | Andesite | Pyroxene andesite | Andesite | Dacite | Dacite | Dacite |
| Analyses as reported (wt percent) | | | | | | | | | |
| $SiO_2$ | 58.23 | 58.12 | 57.75 | 58.40 | 59.95 | 61.17 | 63.99 | 63.33 | 66.53 |
| $TiO_2$ | 1.72 | 1.49 | 1.51 | 1.62 | 0.92 | 1.33 | 1.06 | 0.80 | 0.83 |
| $Al_2O_3$ | 14.85 | 15.25 | 15.53 | 15.16 | 16.25 | 15.15 | 14.98 | 14.27 | 15.23 |
| $Fe_2O_3$ | 9.35 | 8.97 | 8.31 | 8.92 | 5.63 | 7.42 | 5.94 | 5.74 | 3.20 |
| FeO | --- | --- | --- | --- | --- | --- | --- | --- | --- |
| MnO | 0.19 | 0.15 | 0.22 | 0.16 | 0.11 | 0.14 | 0.12 | 0.12 | 0.07 |
| MgO | 2.40 | 2.98 | 2.77 | 2.58 | 2.76 | 2.10 | 1.28 | 0.95 | 0.66 |
| CaO | 5.52 | 5.85 | 6.18 | 5.67 | 6.10 | 4.78 | 3.72 | 3.29 | 3.04 |
| $Na_2O$ | 4.11 | 3.94 | 3.73 | 3.96 | 3.19 | 4.15 | 4.29 | 4.36 | 4.57 |
| $K_2O$ | 1.63 | 1.28 | 1.03 | 1.56 | 1.59 | 1.73 | 1.74 | 1.92 | 2.39 |
| $P_2O_5$ | 0.70 | 0.40 | 0.35 | 0.39 | 0.21 | 0.42 | 0.35 | 0.25 | 0.22 |
| LOI | 1.21 | 1.66 | 2.08 | 1.14 | 2.90 | 0.89 | 2.03 | 4.23 | 2.73 |
| Total | 99.90 | 100.07 | 99.47 | 99.55 | 99.61 | 99.27 | 99.49 | 99.25 | 99.47 |
| Analyses recalculated volatile-free and normalized to 100% with all Fe as FeO (wt percent) | | | | | | | | | |
| $SiO_2$ | 59.57 | 59.60 | 59.81 | 59.89 | 62.35 | 62.65 | 66.06 | 67.06 | 69.00 |
| $TiO_2$ | 1.76 | 1.52 | 1.56 | 1.66 | 0.96 | 1.36 | 1.09 | 0.84 | 0.86 |
| $Al_2O_3$ | 15.19 | 15.64 | 16.08 | 15.54 | 16.90 | 15.51 | 15.46 | 15.10 | 15.80 |
| FeO* | 8.60 | 8.27 | 7.75 | 8.23 | 5.27 | 6.84 | 5.51 | 5.47 | 2.98 |
| MnO | 0.19 | 0.15 | 0.23 | 0.16 | 0.11 | 0.14 | 0.13 | 0.13 | 0.08 |
| MgO | 2.46 | 3.05 | 2.87 | 2.64 | 2.87 | 2.15 | 1.32 | 1.00 | 0.69 |
| CaO | 5.65 | 6.00 | 6.40 | 5.82 | 6.35 | 4.89 | 3.84 | 3.48 | 3.15 |
| $Na_2O$ | 4.20 | 4.04 | 3.86 | 4.06 | 3.32 | 4.25 | 4.43 | 4.61 | 4.74 |
| $K_2O$ | 1.67 | 1.31 | 1.07 | 1.59 | 1.66 | 1.78 | 1.80 | 2.03 | 2.48 |
| $P_2O_5$ | 0.72 | 0.41 | 0.37 | 0.40 | 0.22 | 0.43 | 0.36 | 0.27 | 0.23 |
| Mg# | 37.5 | 43.6 | 43.8 | 40.2 | 53.3 | 39.8 | 33.4 | 27.7 | 32.6 |
| Modes (volume percent) | | | | | | | | | |
| Plagioclase | 1.4 | 6.1 | 2.1 | 0.5 | 17.6 | 0.3 | 4.1 | 3.6 | 2.6 |
| Clinopyroxene | 0.1 | 1.1 | 0.2 | 0.1 | 4.0 | 0.1 | 0.4 | 0.6 | 0.7 |
| Orthopyroxene | 0.1 | --- | 0.4 | --- | 2.8 | --- | 0.2 | 0.4 | --- |
| Olivine | --- | 0.5 | trace | --- | --- | --- | --- | 0.3 | --- |
| Fe-Ti Oxide | trace | 0.1 | trace | trace | 0.1 | 0.1 | 0.4 | 0.5 | 0.1 |
| Hornblende | --- | --- | --- | --- | --- | --- | --- | --- | --- |
| Quartz | --- | --- | --- | --- | --- | --- | --- | --- | --- |
| K-feldspar | --- | --- | --- | --- | --- | --- | --- | --- | --- |
| Other | --- | --- | --- | --- | --- | --- | --- | --- | --- |
| | --- | --- | --- | --- | --- | --- | --- | --- | --- |
| Groundmass | 98.4 | 92.2 | 97.3 | 99.4 | 75.5 | 99.5 | 94.9 | 94.6 | 96.6 |
| No. points counted | 776 | 800 | 802 | 814 | 744 | 750 | 691 | 812 | 794 |
| Texture (rock/ groundmass) | sparsely phyric/ pilotaxitic | porphyritic/ pilotaxitic | sparsely phyric/ intergranular | sparsely phyric/ hyalopilitic | porphyritic/ hyalopilitic | sparsely phyric/ pilotaxitic | porphyritic/ pilotaxitic | porphyritic/ pilotaxitic | sparsely phyric/ pilotaxitic |
| Trace element analyses (ppm) | | | | | | | | | |
| Ba | 336 | 245 | 238 | 298 | 360 | 331 | 343 | 409 | 430 |
| Rb | 43 | 24 | 21 | 35 | 46 | 33 | 33 | 54 | 54 |
| Sr | 332 | 330 | 333 | 326 | 397 | 298 | 279 | 269 | 239 |
| Y | 41 | 31 | 31 | 29 | 26 | 45 | 38 | 42 | 35 |
| Zr | 292 | 225 | 231 | 244 | 248 | 352 | 288 | 385 | 346 |
| Nb | 19 | 18 | 15 | 21 | 16 | 25 | 21 | 23 | 23 |
| Ni | --- | --- | 17 | 11 | --- | --- | --- | <10 | --- |
| Cu | --- | --- | 155 | 82 | --- | --- | --- | 24 | --- |
| Zn | --- | --- | 87 | 93 | --- | --- | --- | 87 | --- |
| Cr | --- | --- | --- | --- | --- | --- | --- | --- | --- |

**Table 1.** Chemical analyses of volcanic and intrusive rocks, Woodland 7.5' quadrangle—Continued

| Map No. | 37 | 38 | 39 | 40 | 41 | 42 | 43 | 44 | 45 |
|---|---|---|---|---|---|---|---|---|---|
| Field sample No. | 97LC-Q57A | 98LC-Q194 | 97LC-Q32 | 97LC-Q105 | 98LC-Q233 | 97LC-Q56 | 97LC-Q144 | 97LC-Q117 | 98LC-Q265 |
| Latitude (N) | 45°53.73' | 45°59.01' | 45°57.78' | 45°57.92' | 45°57.24' | 45°54.16' | 45°58.02' | 45°57.05' | 45°53.30' |
| Longitude (W) | 122°43.07' | 122°39.24' | 122°43.00' | 122°40.48' | 122°39.75' | 122°43.84' | 122°44.02' | 122°43.57' | 122°43.04' |
| Map unit | Td | Td | Tiba | Tiba | Tiba | Tia | Tia | Tia | Tbh |
| Rock type | Dacite | Dacite | Basaltic andesite | Hypersthene basaltic andesite | Basaltic andesite | Basaltic andesite | Andesite | Andesite | Hyaloclastite |
| Analyses as reported (wt percent) | | | | | | | | | |
| $SiO_2$ | 67.47 | 65.68 | 52.05 | 52.27 | 54.36 | 55.68 | 55.81 | 56.23 | 51.38 |
| $TiO_2$ | 0.59 | 0.35 | 0.84 | 1.52 | 0.99 | 1.64 | 1.69 | 1.24 | 1.90 |
| $Al_2O_3$ | 14.57 | 13.00 | 17.06 | 17.17 | 17.27 | 15.77 | 15.62 | 16.23 | 13.85 |
| $Fe_2O_3$ | 4.54 | 3.30 | 8.01 | 9.54 | 8.15 | 10.36 | 9.73 | 8.61 | 13.30 |
| FeO | --- | --- | --- | --- | --- | --- | --- | --- | --- |
| MnO | 0.12 | 0.07 | 0.13 | 0.16 | 0.12 | 0.16 | 0.17 | 0.13 | 0.18 |
| MgO | 0.70 | 0.47 | 7.42 | 4.58 | 5.43 | 3.41 | 3.40 | 4.02 | 2.96 |
| CaO | 2.54 | 4.69 | 9.56 | 8.55 | 8.11 | 7.15 | 6.98 | 7.68 | 6.42 |
| $Na_2O$ | 5.03 | 2.45 | 2.41 | 3.18 | 2.96 | 3.97 | 3.58 | 3.50 | 2.13 |
| $K_2O$ | 2.20 | 0.32 | 0.58 | 1.00 | 0.90 | 0.85 | 1.43 | 1.13 | 0.88 |
| $P_2O_5$ | 0.15 | 0.08 | 0.19 | 0.31 | 0.21 | 0.30 | 0.34 | 0.30 | 0.27 |
| LOI | 1.74 | 9.02 | 1.66 | 1.58 | 1.44 | 0.64 | 1.04 | 0.81 | 6.15 |
| Total | 99.65 | 99.43 | 99.92 | 99.85 | 99.92 | 99.92 | 99.78 | 99.87 | 99.42 |
| Analyses recalculated volatile-free and normalized to 100% with all Fe as FeO (wt percent) | | | | | | | | | |
| $SiO_2$ | 69.23 | 72.91 | 53.41 | 53.72 | 55.66 | 56.67 | 57.09 | 57.26 | 55.89 |
| $TiO_2$ | 0.61 | 0.39 | 0.87 | 1.57 | 1.02 | 1.67 | 1.72 | 1.26 | 2.06 |
| $Al_2O_3$ | 14.95 | 14.43 | 17.50 | 17.64 | 17.68 | 16.05 | 15.97 | 16.53 | 15.06 |
| FeO* | 4.19 | 3.30 | 7.40 | 8.82 | 7.51 | 9.49 | 8.95 | 7.89 | 13.02 |
| MnO | 0.12 | 0.08 | 0.13 | 0.16 | 0.12 | 0.16 | 0.18 | 0.14 | 0.20 |
| MgO | 0.71 | 0.52 | 7.62 | 4.70 | 5.56 | 3.47 | 3.47 | 4.09 | 3.22 |
| CaO | 2.61 | 5.21 | 9.81 | 8.78 | 8.30 | 7.28 | 7.14 | 7.82 | 6.99 |
| $Na_2O$ | 5.16 | 2.72 | 2.47 | 3.26 | 3.03 | 4.04 | 3.66 | 3.57 | 2.31 |
| $K_2O$ | 2.26 | 0.36 | 0.60 | 1.02 | 0.92 | 0.86 | 1.46 | 1.15 | 0.95 |
| $P_2O_5$ | 0.15 | 0.09 | 0.19 | 0.32 | 0.21 | 0.31 | 0.35 | 0.31 | 0.30 |
| Mg# | 26.3 | 24.8 | 68.4 | 52.8 | 60.8 | 43.4 | 44.9 | 52.1 | 34.2 |
| Modes (volume percent) | | | | | | | | | |
| Plagioclase | 8.6 | 5.1 | 25.9 | 40.3 | 47.7 | 0.4 | 1.6 | 0.5 | - |
| Clinopyroxene | 0.4 | 0.9 | 2.5 | 0.3 | 0.8 | 0.1 | 0.6 | 0.1 | - |
| Orthopyroxene | 0.9 | 0.3 | - | 8.0 | 10.3 | - | 0.3 | - | - |
| Olivine | - | 0.1 | 4.8 | - | 0.8 | - | - | - | - |
| Fe-Ti Oxide | 0.4 | 0.3 | - | - | - | - | trace | - | - |
| Hornblende | - | - | - | - | - | - | - | - | - |
| Quartz | - | - | - | - | - | - | - | - | - |
| K-feldspar | - | - | - | - | - | - | - | - | - |
| Other | - | - | - | - | - | - | - | - | - |
| Groundmass | 89.7 | 93.3 | 66.8 | 51.4 | 40.4 | 99.5 | 97.5 | 99.4 | 100.0 |
| No. points counted | 789 | 796 | 733 | 777 | 750 | 777 | 765 | 790 | --- |
| Texture (rock/ groundmass) | porphyritic/ hyalopilitic | porphyritic/ hyalopilitic | seriate/ intergranular | porphyritic/ intersertal | seriate/ intergranular | sparsely phyric/ pilotaxitic | sparsely phyric/ pilotaxitic | sparsely phyric/ pilotaxitic | fragmental |
| Trace element analyses (ppm) | | | | | | | | | |
| Ba | 401 | 578 | 243 | 252 | 187 | 203 | 277 | 229 | 455 |
| Rb | 45 | 13 | 19 | 31 | 18 | 29 | 31 | 23 | 26 |
| Sr | 188 | 582 | 530 | 464 | 373 | 357 | 323 | 345 | 272 |
| Y | 43 | 43 | 15 | 25 | 19 | 24 | 34 | 22 | 31 |
| Zr | 406 | 482 | 124 | 183 | 137 | 171 | 275 | 228 | 169 |
| Nb | 27 | 23 | 12 | 11 | 10 | 15 | 18 | 18 | 15 |
| Ni | --- | <10 | --- | --- | 67 | --- | --- | --- | 32 |
| Cu | --- | 23 | --- | --- | 119 | --- | --- | --- | 34 |
| Zn | --- | 58 | --- | --- | 67 | --- | --- | --- | 124 |
| Cr | --- | --- | --- | --- | --- | --- | --- | --- | --- |

**Table 1.** Chemical analyses of volcanic and intrusive rocks, Woodland 7.5' quadrangle—Continued

| Map No. | 46 | 47 | 48 | 49 | 50 | 51 | 52 | 53 | 54 |
|---|---|---|---|---|---|---|---|---|---|
| Field sample No. | 97LC-Q78A* | 97LC-Q78C* | 97LC-Q65A* | 97LC-Q65B* | 97LC-Q64C* | 97LC-Q67A* | 97LC-Q64A* | 97LC-Q64B* | 99LC-Q317* |
| Latitude (N) | 45°53.44' | 45°53.41 | 45°53.98' | 45°53.98' | 45°53.94' | 45°53.92' | 45°53.88 | 45°53.82 | 45°53.72' |
| Longitude (W) | 122°43.22' | 122°43.03 | 122°42.53' | 122°42.53' | 122°43.20' | 122°43.64' | 122°43.20 | 122°42.96 | 122°43.01' |
| Map unit | Tggc(?) | Tggc(?) | Tggc(?) | Tggc(?) | Tgww | Tgww | Tgsb | Tgsb | Tgsb |
| Rock type | Basaltic andesite | Basaltic andesite | Basaltic andesite | Basaltic andesite | Basaltic andesite | Basaltic andesite | Basaltic andesite | Basaltic andesite | Basaltic andesite |
| Analyses as reported (wt percent) | | | | | | | | | |
| $SiO_2$ | 54.21 | 54.80 | 55.80 | 56.40 | 55.45 | 55.60 | 53.52 | 53.45 | 54.53 |
| $TiO_2$ | 1.84 | 1.90 | 1.96 | 1.98 | 2.00 | 2.01 | 1.94 | 1.79 | 1.84 |
| $Al_2O_3$ | 14.35 | 14.77 | 15.56 | 15.44 | 13.78 | 13.95 | 13.72 | 14.07 | 14.22 |
| $Fe_2O_3$ | --- | --- | --- | --- | --- | --- | --- | --- | --- |
| FeO | 10.03 | 8.89 | 7.37 | 7.25 | 11.35 | 10.78 | 11.64 | 10.90 | 11.00 |
| MnO | 0.22 | 0.25 | 0.14 | 0.14 | 0.20 | 0.20 | 0.21 | 0.21 | 0.18 |
| MgO | 4.02 | 3.93 | 4.08 | 3.91 | 3.66 | 3.62 | 4.67 | 4.60 | 4.29 |
| CaO | 9.10 | 8.78 | 8.27 | 8.54 | 7.20 | 7.32 | 8.51 | 8.51 | 8.27 |
| $Na_2O$ | 2.96 | 3.03 | 2.98 | 3.12 | 3.12 | 3.40 | 2.97 | 2.94 | 2.76 |
| $K_2O$ | 1.50 | 1.53 | 1.57 | 1.63 | 1.81 | 1.61 | 1.27 | 1.27 | 1.27 |
| $P_2O_5$ | 0.35 | 0.37 | 0.37 | 0.38 | 0.35 | 0.36 | 0.30 | 0.34 | 0.35 |
| LOI | --- | --- | --- | --- | --- | --- | --- | --- | --- |
| Total | 98.59 | 98.24 | 98.10 | 98.80 | 98.92 | 98.85 | 98.74 | 98.09 | 98.71 |
| Analyses recalculated volatile-free and normalized to 100% with all Fe as FeO (wt percent) | | | | | | | | | |
| $SiO_2$ | 54.99 | 55.78 | 56.88 | 57.09 | 56.05 | 56.25 | 54.20 | 54.49 | 55.25 |
| $TiO_2$ | 1.87 | 1.93 | 2.00 | 2.00 | 2.02 | 2.03 | 1.96 | 1.83 | 1.86 |
| $Al_2O_3$ | 14.56 | 15.03 | 15.86 | 15.63 | 13.93 | 14.11 | 13.89 | 14.34 | 14.41 |
| FeO* | 10.18 | 9.05 | 7.51 | 7.34 | 11.47 | 10.90 | 11.79 | 11.11 | 11.15 |
| MnO | 0.22 | 0.26 | 0.14 | 0.15 | 0.20 | 0.20 | 0.21 | 0.22 | 0.18 |
| MgO | 4.08 | 4.00 | 4.16 | 3.96 | 3.70 | 3.66 | 4.73 | 4.69 | 4.35 |
| CaO | 9.23 | 8.94 | 8.43 | 8.64 | 7.28 | 7.41 | 8.62 | 8.68 | 8.38 |
| $Na_2O$ | 3.00 | 3.08 | 3.04 | 3.16 | 3.15 | 3.44 | 3.01 | 3.00 | 2.80 |
| $K_2O$ | 1.52 | 1.56 | 1.60 | 1.65 | 1.83 | 1.63 | 1.29 | 1.29 | 1.29 |
| $P_2O_5$ | 0.36 | 0.37 | 0.38 | 0.39 | 0.36 | 0.37 | 0.30 | 0.35 | 0.35 |
| Mg# | 45.7 | 48.1 | 53.7 | 53.1 | 40.4 | 41.3 | 45.7 | 47.0 | 45.0 |
| Modes (volume percent) | | | | | | | | | |
| Plagioclase | - | - | - | - | - | - | - | - | - |
| Clinopyroxene | - | - | - | - | - | - | - | - | - |
| Orthopyroxene | - | - | - | - | - | - | - | - | - |
| Olivine | - | - | - | - | - | - | - | - | - |
| Fe-Ti Oxide | - | - | - | - | - | - | - | - | - |
| Hornblende | - | - | - | - | - | - | - | - | - |
| Quartz | - | - | - | - | - | - | - | - | - |
| K-feldspar | - | - | - | - | - | - | - | - | - |
| Other | - | - | - | - | - | - | - | - | - |
| Groundmass | 100.0 | 100.0 | 100.0 | 100.0 | 100.0 | 100.0 | 100.0 | 100.0 | 100.0 |
| No. points counted | --- | --- | --- | --- | --- | --- | --- | --- | --- |
| Texture (rock/groundmass) | aphyric/intersertal | aphyric/intersertal | aphyric/intersertal | microphyric/intersertal | microphyric/intersertal | aphyric/intergranular | aphyric/intergranular | microphyric/intersertal | microphyric/intersertal |
| Trace element analyses (ppm) | | | | | | | | | |
| Ba | 583 | 829 | 940 | 763 | 695 | 703 | 442 | 575 | 645 |
| Rb | 34 | 37 | 40 | 40 | 44 | 38 | 30 | 34 | 33 |
| Sr | 324 | 346 | 372 | 357 | 321 | 331 | 308 | 314 | 317 |
| Y | 36 | 38 | 54 | 59 | 36 | 35 | 32 | 36 | 46 |
| Zr | 167 | 172 | 179 | 181 | 169 | 174 | 154 | 167 | 164 |
| Nb | 11.1 | 11.6 | 11 | 13.7 | 12.8 | 13.6 | 13.4 | 12.6 | 12.1 |
| Ni | 16 | 8 | 12 | 9 | 9 | 4 | 5 | 16 | 9 |
| Cu | 27 | 28 | 27 | 30 | 23 | 23 | 24 | 26 | 29 |
| Zn | 121 | 127 | 141 | 137 | 118 | 119 | 117 | 114 | 115 |
| Cr | 51 | 49 | 50 | 54 | 26 | 32 | 38 | 49 | 46 |

**Table 2**. Comparison of selected chemical and paleomagnetic characteristics of Grande Ronde Basalt flows in the Woodland and Ridgefield quadrangles (R.C. Evarts, unpub. data; J.T. Hagstrum, written commun., 1999, 2000, 2001)

[Magnetic polarity: N, normal; R, reversed. Paleomagnetic directions determined by standard laboratory alternating-field demagnetization techniques; terminology is that of Wells and others (1989). Ranges in chemical composition based on analyses recalculated volatile-free and normalized to 100% with all Fe as FeO]

| Map unit | Tgsb | Tgww | Tggc(?) |
|---|---|---|---|
| Magnetic polarity | N | N | R |
| Paleomagnetic direction | north | shallow northeast | south-southwest |
| MgO (wt %) | 4.35-4.82 | 3.66-3.70 | 3.96-4.16 |
| $TiO_2$ (wt %) | 1.82-1.99 | 2.02-2.03 | 1.87-2.00 |
| $P_2O_5$ (wt %) | 0.30-0.35 | 0.36-0.40 | 0.36-0.39 |
| CaO (wt %) | 8.38-8.87 | 7.28-7.41 | 8.43-9.23 |
| $K_2O$ (wt %) | 1.23-1.29 | 1.63-1.83 | 1.49-1.65 |
| Ba (ppm) | 442-645 | 693-703 | 583-940 |
| Cr (ppm) | 38-51 | 26-32 | 49-54 |